國立臺灣大學生命科學院生化科學研究所

碩士論文

Graduate Institute of Biochemical Sciences

College of Life Science

National Taiwan University

Master Thesis

探討酪胺酸去磷酸酶 N3 調控 Bicaudal D 之分子機制

Molecular regulation of Bicaudal D protein

by tyrosine phosphatase PTPN3

張雅閔

Ya-Min Chang

指導教授：陳光超 博士

Advisor: Guang-Chao Chen, Ph.D.

中華民國 107 年 7 月

July, 2018

國立臺灣大學碩士學位論文

口試委員會審定書

探討酪胺酸去磷酸酶 N3 調控 Bicaudal D 之分子機制

Molecular regulation of Bicaudal D protein

by tyrosine phosphatase PTPN3

　　本論文係張雅閔君（學號 R05B46014）在國立臺灣大學生化科學研究所完成之碩士學位論文，於民國 107 年 07 月 25 日承下列考試委員審查通過及口試及格，特此證明。

口試委員：

_____（簽名）（召集人）

_____

_____

_____（指導教授）

I

中文摘要

酪氨酸磷酸化在細胞分化、細胞增生與遷移中扮演重要的角色，其受到蛋白質酪氨酸磷酸酶 (Protein tyrosine kinases；PTKs)與蛋白質酪氨酸去磷酸酶 (protein tyrosine phosphatases；PTPs)相互調節。我們過去發表文獻提出 PTPN3 參與在調控 EGFR 內吞的運送過程與肺癌細胞的增生。PTPN3 為一非受體型蛋白質酪氨酸去磷酸酶，其中 N 端有一 FERM 區域，中間有 PDZ 區域，而 C 端有一 PTP 活性區域。然而，PTPN3 仍有許多生物性功能尚未釐清。

為了更近一步探討 PTPN3 功能，我們利用質譜尋找 PTPN3 的可能受質，結果發現 Bicaudal D 蛋白(BICD)是其中一個可能性受質。BICD 是動力蛋白(dynein)的接頭蛋白，與小 GTP 酶 Rab6 具有交互作用，且藉由徵招動力蛋白-動力激活蛋白 (Dynactin)複合物調節內質網和高基氏體間的運送。在此篇論文中，我們發現 BICD 是會被酪氨酸磷酸化的蛋白，並且 PTPN3 可以降低 BICD 酪氨酸磷酸化的程度。此外，實驗結果也顯示 Src 酪氨酸激酶可以酪氨酸磷酸化 BICD 的卷曲螺旋功能區域中的酪氨酸。而且也發現 BICD 酪氨酸突變對於水泡性口炎病毒膜蛋白(VSVG)的順行性運輸無顯著影響。在果蠅方面，發現果蠅 Ptpmeg 與果蠅 BicD 具有基因遺傳交互作用。

此外，我們目前也著手探討果蠅 BicD 一些與 Ptpmeg 相關的生理功能。

關鍵詞：酪氨酸磷酸化、PTPN3、BICD、Src

Abstract

Protein tyrosine phosphorylation plays a critical role in cell signaling and regulates a variety of biological processes, including cell differentiation, migration and proliferation. The molecular switch of tyrosine phosphorylation is coordinated by protein tyrosine kinases (PTKs) and protein tyrosine phosphatases (PTPs). Our previous study has shown that PTPN3 is involved in the regulation of EGFR endocytic trafficking and lung cancer cell proliferation. PTPN3 is a non-transmembrane PTP that contains a N-terminal FERM domain, a PDZ domain and the C-terminal PTP domain. However, the biological function of PTPN3 remains largely unknown.

Previously, we used substrate trapping approach to find the potential substrates of PTPN3. The results showed that Bicaudal D (BICD) is a potential substrate of PTPN3. BICD, a dynein adaptor protein, interacts with the small GTPase Rab6 and recruits the dynein-dynactin complex to regulate Golgi-ER transport. In this study, we found that the BICD is a tyrosine phosphorylated protein and PTPN3 can down-regulate the phospho-tyrosine level of BICD. Moreover, Src tyrosine kinase can phosphorylate the tyrosine residues in the coiled-coil domain of BICD. Further, our preliminary data showed that BICD-YF mutant does not affect the anterograde transport of VSVG and the Golgi morphology. In *Drosophila*, we found that dPtpmeg genetically interacts with dBicD. We are currently investigating the function of dPtpmeg-dBicD interaction in Drosophila development.
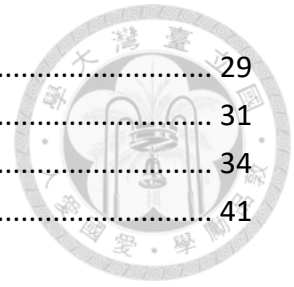
Key words: PTPN3, BICD2, tyrosine phosphorylation, Src

Content

Introduction

Protein tyrosine phosphatase

PTP overview

Protein tyrosine phosphorylation coordinated by protein tyrosine kinases (PTKs) and protein tyrosine phosphatases (PTPs) plays a critical role in cell signaling and regulates a variety of biological processes, including cell differentiation, migration and proliferation (Ostman and Bohmer, 2001; Tonks, 2006). PTPs are a superfamily of enzymes that remove phosphate group from phosphorylated Tyr, Ser/ Thr residues on proteins, and even phospholipid (Maehama and Dixon, 1998). PTPs were initially considered as housekeeping enzymes with constitutive activity to dephosphorylate every substrate they were confronted(Angers-Loustau et al., 1999). About 100 PTP-superfamily genes in human genome (Alonso et al., 2004). Characterized by the active-site signature sequence $HC(X)_5R$ in the conserved catalytic domain, in which cysteine residue is to be a nucleophile and necessary for catalysis, PTPs can be divided into two major groups: the classical tyrosine-specific phosphatases and the dual-specificity phosphatases (DUSPs). Classical PTPs only can dephosphorylate phosphotyrosine residue on proteins; and DUSPs can accommodate the phosphotyrosine, phosphoserine, and phosphothreonine residues on proteins, in addition to inositol phospholipids. PTEN, a DUSP, is a well-known tumor suppressor that have been

implicated in insulin signaling and cell death through anoikis by dephosphorylating PIP_3 and Akt (Maehama and Dixon, 1998; Yamada and Araki, 2001).
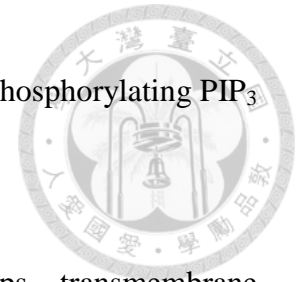
Classical PTPs can be further categorized into two groups, transmembrane receptor-like PTPs (RPTPs) and non-transmembrane PTPs (NRPTPs) (Andersen et al., 2004). RPTPs regulate signaling transduction through the ligand-dependent protein tyrosine dephosphorylation, and many of them have been reported to be involved in the regulation of cell-cell and cell-matrix adhesions. For instance, CD45, a RPTP, acts as a vital role in the immune system that regulates the initiation of T and B cell receptor signaling by dephosphorylating Src family protein-tyrosine kinases such as Lck and Fyn, and also involves in autoimmune response (Beltran and Bixby, 2003; Katagiri et al., 1999; Lee et al., 1996; Rheinlander et al., 2018). On the other hand, many non-transmembrane PTPs participate in regulating growth factor signaling pathways (Tonks, 2006). NRPTPs have a single PTP domain and all kinds of non-catalytic regulatory domains with different functions, including controlling the NRPTPs′ activity by different protein-protein interactions at the active site or by modulating substrate specificity, and also regulating NRPTPs subcellular distribution, which causes the indirect change of NRPTPs activity by restricting interacts to special substrates at unique location (Garton et al., 1997; Tonks, 2006). For example, classical NRPTP PTP1B is a negative regulator of insulin response, and involves in integrin signaling
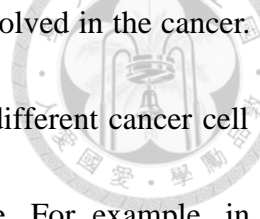
(Cheng et al., 2002; Liu et al., 1998).

The balance of protein tyrosine phosphorylation is important for various cellular regulatory processes. Abnormal tyrosine phosphorylation level affects metabolism, the immune response and causes disease such as diabetes, cancers (Hendriks et al., 2013; Motiwala and Jacob, 2006).

PTPN3

Protein tyrosine phosphatase non-receptor type 3 (PTPN3), also called PTPH1, is a member of non-receptor type classical PTPs (Tonks, 2006). It contains a N-terminal FERM (Band *4*.1, *e*zrin, *r*adixin, *m*oesin homology) domain, a PDZ (PSD-95, Dlg, ZO-1) domain and the C-terminal PTP domain (Bretscher et al., 2002; Edwards et al., 2001). The FERM domain was identified in band 4.1 at first, and has been well estimated in the ERM proteins, the focal adhesion protein talin and Protein 4.1 (Chishti et al., 1998; Leto and Marchesi, 1984). It acts as a linker role to bind with membrane-associated or transmembrane proteins, and thought to be possible regulate the pathways of actin cytoskeleton (Wadham et al., 2000). The PDZ domain is to modulate the protein-protein interaction (Hung and Sheng, 2002), and is often discovered in scaffolding proteins, therefore its associated partners are specific proteins at the specialized locations in the cell (Kim and Sheng, 2004). The PTP domain is catalytic domain for PTPs activity.
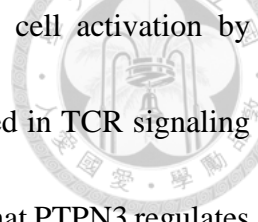
Recently, more and more studies have reported that PTPN3 is involved in the cancer. PTPN3 can both play the oncogenic role and tumor suppressor in different cancer cell lines, which may be dependent on tissue, species, and substrate. For example, in tumorgenesis, Hou et al. revealed that PTPN3 directly binds with a Ras effector, p38γ MAPK, by the PDZ domain, and then dephosphorylates p38γ to induce Ras-mediated oncogenesis in colon cancer (Hou et al., 2010). Overexpression of PTPN3 increases cell proliferation and migration in intrahepatic cholangiocarcinoma (ICC) cell lines and correlates with bad clinical outcome (Gao et al., 2014). Besides this, the two mutations of PTPN3, L232R and L384H, which were often found in ICC samples, are thought to be gain-of-function mutations and related to clinical outcome (Gao et al., 2014).

On the other hand, in tumor suppression, overexpression of PTPN3 in mouse NIH3T3 cells lead to inhibit cell growth and cell-cycle progression through dephosphorylation of VCP (p97/CDC48), which is an important cell cycle regulator (Zhang et al., 1999). Zhang et al. also discovered that PTPN3 binds with 14-3-3β phosphoserine-binding protein, which might be an adaptor protein and a linker between serine/threonine and tyrosine phosphorylation-dependent signaling pathways (Zhang et al., 1997). In addition, ectopic expression of PTPN3 led to decrease the colony formation in NSCLC cell lines (Jung et al., 2012).

Apart from the role of PTPN3 in cancer, Han et al. discovered that PTPN3 is also
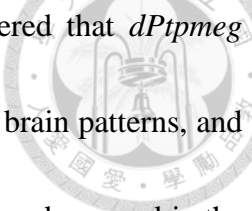
involved in T cell antigen receptor signaling. PTPN3 abolishs T cell activation by

dephosphorylating membrane-associated proteins, which are involved in TCR signaling

in Jurkat T cells (Han et al., 2000). Therefore, Pilecka et al. reported that PTPN3 regulates

growth hormone receptor signaling by the secretion of insulin-like growth factor 1, is

often related with sexual size dimorphism (Chase et al., 2005; Pilecka et al., 2007).

In our previous study, PTPN3 plays a tumor suppressor by accelerating EGFR

endocytic degration to inhibit the proliferation and migration in NSCLC cells. We found

Eps15, a multidomain adaptor protein that is involved in endocytic trafficking, is a

substrate of PTPN3 (Li et al., 2015). In addition, we also discovered that Eps15b is a

substrate of PTPN3. The study provides a novel role of PTPN3 in endosomal sorting

and endocytic trafficking. In this study, to further understand the role of PTPN3, we

performed Mass spectrometry-based substrate trapping strategy, and found that BICD2

is the potential substrates of PTPN3. BICD2, a dynein adaptor protein, interacts with the

small GTPase Rab6 and recruits the dynein-dynactin complex to regulate Golgi-ER

transport and plays a critical role in intracellular transport. So, we want to investigate

that potential role of PTPN3 in intracellular transport by regulating the PTM of BICD2.

dPtpmeg

Drosophila Ptpmeg (dPtpmeg), one of the *Drosophila* non-transmembrane PTPs,

containing a N-terminal FERM domain, a PDZ domain and the C-terminal PTP domain

(Bretscher et al., 2002; Edwards et al., 2001). Whited et al. discovered that *dPtpmeg* mutants disrupt the projections of mushroom body (MB) in the adult brain patterns, and also the thickness and length of the dorsally projecting MB lobes were decreased in the adult flies (Whited et al., 2007). Moreover, our previous study showed that the migration rate of border cells was accelerated, and the cluster compassed the oocyte prematurely at stage 9 in *dPtpmeg* mutant (Li et al., 2015). The role of dPtpmeg is a negative regulator in the EGFR/Ras/MAPK signaling pathway during *Drosophila* wing morphogenesis. Li et al. also found Eps 15, the substrate of dPtpmeg, involves in the EGFR signaling pathway. Besides these, the molecular function of dPtpmeg remains largely unknown.

Intracellular transport

Intracellular transport overview

Transport of different intracellular cargoes such as proteins, vesicles, RNA, and organelles, along cytoskeleton filaments is essential for the cellular function. The basic mechanism of regulating intracellular transport is well-known and highly conserved in different cell types. The system of cytoskeleton filament contains microtubules, which is for long-term movement, and actin, which is for relatively short-distance transport (Titus, 2018). According to the cargo and its target site, three major groups of motor proteins - kinesins, dyneins, and myosins – have been identified to regulate the intracellular trafficking along microtubules (Hirokawa, 1998; Karki and Holzbaur, 1999; Vale, 2003). The myosin motor proteins move along microfilaments, and are also important for cell movement. Generally, each type of motor protein moves in a single direction on microtubules. Kinesins mobile anterogradely to the plus end and myosins move towards the minus end. Some of cargos translocate unidirectionally, interestingly, some of them such as protein complexes and many organelles present towards the plus and minus end movements to transport to the hard-arriving targets or distant destination by the multiple activities of several different motor proteins. For example, several reports have implicated that kinesin and dynein motor proteins can simultaneously stay stably interacted with the cargos, even they are inactive (Hancock, 2014; Welte, 2004).
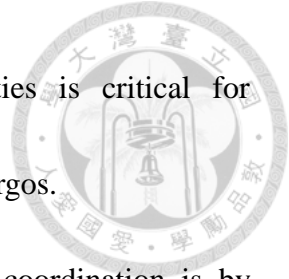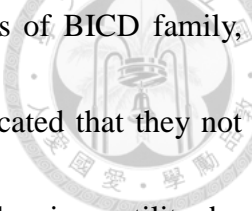
The balance between the converse kinesin and dynein activities is critical for modulating the transport processing and the proper distribution of cargos.

One way to regulate the cargos transport and motor proteins coordination is by adaptor proteins that connect the motor proteins to cargo (Akhmanova and Hammer, 2010). Motor adaptors, including membrane-associated cargo receptors, signaling molecules and scaffolding factors, often act the important components of the large protein complexes (Schlager and Hoogenraad, 2009). The scaffolding protein JNK-interacting protein 1 (JIP1), one of well-studied adaptor proteins, regulates the bidirectional transport of amyloid precursor protein (APP) in axons by the reversible phosphorylation and the coordination with kinesin and dynein motor proteins (Fu and Holzbaur, 2013). van Spronsen proposes that the TRAK1 regulates the mitochondria transport to axons by linking the kinesin-1 to the mitochondria-anchored protein Miro in neurons, and TRAK2 steer the mitochondria into dendrites by connecting the dynein and Miro (van Spronsen et al., 2013). Other adaptor proteins haven been well-characterized such as Rab7-interacting lysosomal protein (RILP), sorting nexins and glutamate receptor-interacting protein (GRIP). In this study, we focused on BICD2 , a member of conserved Bicaudal D (BICD) proteins family of motor adaptors.
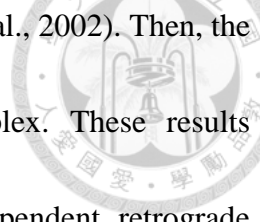
BICD2

Protein bicaudal D homolog 2 (BICD2), one of the adaptor proteins BICD family, has

the multiple functions in microtubule motor proteins. The members of BICD family, including BICD1, BICD2, BICDR1, and BICDR2, have been implicated that they not only can couple dynein motors to cargo but also increase the dynein motility by promoting the interaction between dynein and its cofactor dynactin (McKenney et al., 2014; Schlager et al., 2014). The distribution of BICD2 is diffused the cytoplasm and specially enriched in Golgi, ER regions and recycling endosomes (Hoogenraad et al., 2001). There are many general structural property and functions between mammalian BICD family proteins, such as highly conserved coiled-coil (CC) domains. BICD2 contains five coiled-coil domains, which can group to three distinct regions. The N-terminal two coiled-coil domains (CC1, CC2) interact with microtubules, like dynein, dynactin and kinesin-1 (Hoogenraad et al., 2001; Hoogenraad et al., 2003). The C-terminal coiled-coil domain (CC3) of BICD2 displays the highest level of evolutionary conservation and binds with different partners that decide the localization to cargo proteins (Martinez-Carrera and Wirth, 2015; Terenzio and Schiavo, 2010). In addition, the N-terminal CC1 domain also can bind with the C-terminal CC3 segment to form the auto-inhibited structure, because it avoids associating with others partners such as dynein (Liu et al., 2013; Matanis et al., 2002).
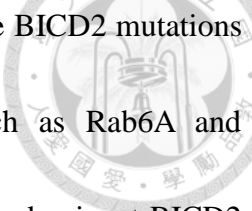
Matanis et al. discovered on early endosome and ER-Golgi vesicles that the C-terminal CC3 of BICD2 directly interacts with the active form of the small GTPase

Rab6A and BICD2 is recuited to trans-Golgi membrane (Matanis et al., 2002). Then, the

N-terminal region of BICD2 recuits the dynein-dynactin complex. These results

indicated that BICD2 plays an important role in in COPI-independent retrograde

transport between Golgi – ER. BICD2 also acts as an adaptor protein binding with

kinesin motors. In the late development stage of neurons, BICD2 replaces BICDR1 and

promotes the anterograde transport of Rab6 exocytic vesicles through the central

coiled-coil domain associates with kinesins, because the expression level of BICDR1 is

decreased (Grigoriev et al., 2007; Schlager et al., 2010). In the G2 phase, Splinter found

that BICD2 interacts with kinesin-1, and facilitates the centrome away from the nucleus.

This showed that BICD2 is critical for mitosis (Splinter et al., 2010). Furthermore,

Jaarsma generated the BICD2 KO mouse, and the mice have the defects of development

in laminar organization of the cerebral cortex, hippocampus and the defects of radial

neuronal migration in cerebellar cortex (Jaarsma et al., 2014). In the study of Dharan et

al., the authors observed that BICD2 promotes the HIV-1 infection through accelerating

the nuclear import of viral cores, and when BICD2 was knockdown, virus sensitized to

detect by innate immune sensing (Dharan et al., 2017).

Moreover, the genetic locus of *BICD2* is related to dominant spinal muscular atrophy

(SMA) (Oates et al., 2013). When theses mutantions of BICD2 caused SMA

overespressed in cells, the morphology of Golgi is fragmented and the localization of

BICD2 is changed (Neveling et al., 2013; Peeters et al., 2013). Some BICD2 mutations lead to impair the association with its interacting partners such as Rab6A and dynein-dynactin (Neveling et al., 2013). The other mutations like the dominant BICD2 mutants have been reported to improve ability to generate DDB complexes, which BICD2 joins dynein with dynactin into a ternary complex, increase retrograde transport and decrease the growth of nurons (Huynh and Vale, 2017). Furthermore, there are several heterozygous mutations of BICD2 have been identified to be induced hereditary spastic paraplegia and autosomal dominant spinal muscular atrophy with lower extremity predominance-2 (SMALED2) (Martinez-Carrera and Wirth, 2015). Martinez-Carrera also discovered that these mutations enhance the stability of microtubules and result in axonal defects in motor neurons (Martinez Carrera et al., 2018).
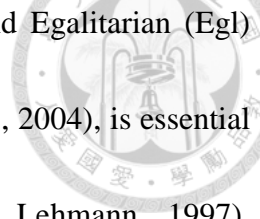
However, about the post-transcriptional modifications (PTMs) of BICD2 are remainly unkown. PTMs of microtubules are believed to regulate the interactions with microtubule-binding parneters. McKenney et al. showed that the detyrosinated α-tubulin decrease the motility of DDB complexes and α-tubulin tyrosine promotes the initial motor–tubulin encounters (McKenney et al., 2016). So, we hope to investigate how the PTM regulates the biological functions of BICD2.
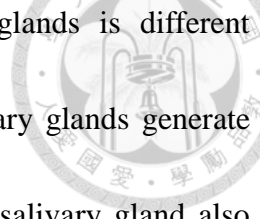
dBicD in fly

Bicaudal-D (BicD) was initially identified in *Drosophila melanogaster* as a regulator of the anterior−posterior polarity in *Drosophila* embryos by the mutant screen of the dominant maternal-effect proteins (Mohler and Wieschaus, 1986). BicD consists of extensive heptad repeats, which modulate the packaging of one helix against another, forming several coiled-coil domains (Bruccoleri et al., 1986). Its distribution is diffused the cytoplasm and enriched at the minus-ends of microtubules (Hoogenraad et al., 2003; Mach and Lehmann, 1997).

The BicD loss-of-function mutations have been show to affect the differentiation of the oocyte, and gain-of-function mutations disrupt the anterior−posterior polarity, which leads to the transformation of the anterior segments into the posterior region, giving rise to a double abdomen, or bicaudal ('two-tailed') embryos (Schupbach and Wieschaus, 1991; Steward, 1987). The null mutations of BicD causes recessive lethality (Ran et al., 1994). Many studies have showed that BicD involves in mRNA transport. For example, during oogenesis, BicD plays a critical role in transporting morphogen mRNAs, the important polarity determinants, to proper subcellular localization, and morphogen mRNAs have been reported including *fs(1)*K10 and *orb* (Swan and Suter, 1996), and *oskar* and *nanos* (Wharton and Struhl, 1989). Also, during embryogenesis, pair-rule transcripts such as *ftz* and *h* are transported by BicD (Bullock and Ish-Horowicz, 2001).

In addition, it was discovered that a complex containing BicD and Egalitarian (Egl) protein, which can interact with motor protein dynein (Navarro et al., 2004), is essential for BicD to determinate the mRNAs localization (Mach and Lehmann, 1997). Furthermore, BicD not only regulates mRNAs but also the organelles localization. Swan et al. found that BicD, dynein and Lissencephaly-1 (Lis1) are involved in positioning the nucleus during oogenesis (Swan et al., 1999). Houalla et al. suggested that Ste-20 like kinase functions with BicD and dynein modulate the migration of nucleus in precursors of R-cells during eye development (Houalla et al., 2005). And, the author further proposed that the process of nuclear transport mat be regulate by reversible phosphorylation of BicD, though the potential mechanism of this modification is unknown. BicD is evolutionarily highly conserved among metazoans, and the relationship between BicD and Rab6 is conserved from mammals to *Drosophila*. Januschke et al. also observed that an interaction between BicD and Rab6 occurs at the Golgi membranes, and regulate the transport of secretory vesicles to affect oocyte polarity (Januschke et al., 2007). Moreover, BicD also mediates the endocytic pathway by transporting the mRNA and protein of clathrin heavy chain into the oocyte during oogenesis (Vazquez-Pianzola et al., 2014). Larsen et al. uncovers a new role for BicD, which involves the bi-directional transport of lipid droplets (Larsen et al., 2008).

Drosophila BicD is also enriched in larval salivary glands (FlyAtlas)

(http://insitu.fruitfly.org/cgi-bin/ex/insitu.pl). The function of salivary glands is different during post-embryonic development. At the larval stage, the salivary glands generate saliva to support food ingestion and intestinal digestion. And the salivary gland also synthesize mucin-type secretory granules termed "glue" granules, containing highly glycosylated glue proteins that are essential for the adhesion of the pupal case to the solid surface during metamorphosis (Beckendorf and Kafatos, 1976; Korge, 1977). The glue proteins transport through the ER and Golgi before forming regulated secretory granules at the TGN (Burgess et al., 2011; Thomopoulos and Kastritsis, 1979). When glue granules are mature, the apical membrane fuse with them, and secrete to the lumen of salivary glands(Biyasheva et al., 2001). After secretion is finished, the granules, which are still at cytoplasm, are degradged by crinophagy, a secretory granule-specific autophagic process (Csizmadia et al., 2018; Harrod and Kastritsis, 1972). Moreover, the larval salivary glands provide an excellent system for genetic analysis to discuss which factors are important to regulate secretory granules process. In this study, we also want to investigate whether *Drosophila* BicD also involves in the transport of glue granules and in which steps.

Material and Methods

Cell culture, transfection and treatments

HEK293T and Neuro2a (N2a) were cultured in DMEM (Dulbecco's modified Eagle's medium) (Invitrogen) supplied with 10% FBS (fetal bovine serum) and P/S (Penicillin/Streptomycin) antibiotics at 37 ℃. PolyJet[TM] DNA In Vitro Transfection Reagents (Signagen) was used for transfection. For cell transfection, the ratio of PolyJet[TM] (μl) and DNA (μl) is 1:2, and dilutes in 200μl serum free medium DMEM respectively. After the diluted solutions were incubated 3 minutes, mixed the diluted PolyJet[TM] reagent and the diluted DNA solution properly, and incubated for 15 minutes in room temperature. At last, the mixture was added into culture dish, then incubated at 37℃ for 24-48 hours.

For experiments required doxycycline treatment, the final concentration of doxycycline was 10μg/ml, and incubated at least 24 hours before performing experiment.

The working concentration of Sodium pervanadate solution was 0.1 mM. Sodium pervanadate stock solution (50 mM) was prepared by mixing equal volumes of 100 mM of H_2O_2 solution and 100 mM Sodium pervanadate solution. Cells were pre-treated 1 hour within fresh medium. Then, Sodium pervanadate was added to medium for 15 minutes.

The working concentration of Src inhibitor Dasatinib (Sigma-Aldrich,CDS023389) was 1μM. And the stock concentration was 5 mM. Cells were pre-treated 1 hour within fresh medium first. Then, Dasatinib was added to medium for 3 hours.
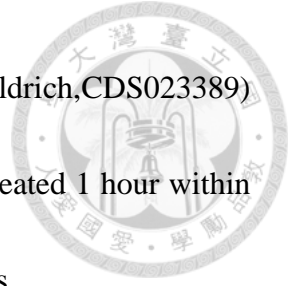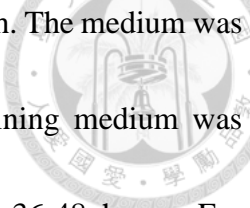
Plasmids and reagents

PTPN3 cDNA was obtained from Open Biosystems (Thermo), pcDNA3.1-HA-PTPN3-WT, DA (D811A), CS (C842S), ΔN (delete residue 1-309), and ΔPTP (delete residue 611-913) were constructed by lab member Dr. Meng-Yen Li. pcDNA3.1-HA-dptpmeg-WT, DA were also constructed by lab member Dr. Meng-Yen Li. The cDNA of mouse BICD2 and fly BicD were obtained from PCR by lab member Jhen-jia Fan. pcDNA3.1-Flag-BICD2-WT, all YF muntants, different truncated forms, and pcDNA3.1-Flag-dBicD were also constructed by lab member Jhen-jia Fan. pRK5-Myc-Src-WT, KD (K296M, Kinase dead) were a generous gift from Dr. Ruey-Hwa Chen (Institute of biochemistry, Academia sinica, Taipei, Taiwan). pcDNA3.1-V5-PTPN3, pcDNA3.1-HA-PTPN3-PDZ (only residue 315-610), pcDNA3.1-Myc-Fyn, and pAS4.1W-Flag-BICD2-WT, Y4F were constructed by myself.

Generation of stable cell line

Delivery of pAS4.1W-Flag-BICD2-WT, Y4F to HEK-293T or N2A cells were performed by lentivirus infection. For lentivirus production, 10 μg of pAS4.1W-Flag-BICD2-WT, Y4F plasmids, 9μg of Δ8.9 plasmids and 2.5μg of VSVG

plasmids were co-infected to HEK-293T cells in the 10 cm culture dish. The medium was

replaced with fresh medium after 24 hours. Then, the virus-containing medium was

collected and filtered with 0.45 μm syring filter after transfecting 36-48 hours. For

lentivirus infection, the medium containing virus was immediately added into N2A cells

along with 8ng/ml polybrene regent. After infection 24-48 hours, the medium was

replaced with fresh medium containing selection marker (puromycin).

Immunoprecipitation and Western blotting

Cells transiently transfected with the indicated plasmids were washed with PBS and

scraped from dishes in IP lysis buffer (50 mM Tris-HCl, pH 7.4, 150 mM NaCl, 1 mM

EDTA, 10% glycerol, 1% Triton X-100) supplied with protease inhibitor cocktail

(Roche) and PhosphoStop (Roche). After collecting the cells into an eppendorf on ice,

cells were lysed by vigorous shacking at 4℃ for 30 minutes and centrifuged for 10

minutes at 13000 rpm. The cell lysate supernatant was harvested and pre-cleaned with

protein G-Sepharose beads (GE Healthcare) for 20-60 minutes and then centrifuged for

5 minutes at 6000 rpm. The supernatant solution was collected in another eppendorf and

incubated with antibody overnight. Afterwards, protein G-Sepharose beads were added

to the cell lysate for one hour at 4℃ and then washed with IP wash buffer (20 mM

Hepes, pH 7.4, 150 mM NaCl, 1.5 mM MgCl, 10% glycerol, 0.01 % Triton X-100) 5

minutes for 3 times. At last, the beads were centrifuged and dried up using a 25 gauge

syringe, with SDS sample buffer added subsequently. Other western blotting samples were harvested by adding SDS sample buffer into culture dish and scraped the cells down.

For western blotting, first IP and other samples were boiled for 10 minutes before loaded into SDS-polyacrylamide gel. Samples were subsequently separated by SDS-polyacrylamide gel electrophoresis and transferred to PVDF membrane (Millipore). The membrane was blocked with 5% milk for 30 minutes at room temperature before indicated antibodies were added and incubated at 4℃ for overnight. The immunoblotting images were visualized by ECL reagents (Millipore).

Immunofluorescence

Cells were seeded on the cover glasses in 6-well culture dish 24~48 hours before performing immunofluorescent staining. First, the cells on the cover glass were gently washed 3 times with PBS and fixed with 4% paraformaldehyde (in PBS) for 15 minutes. Perforation was performing by 5 minutes of PBST (0.1% Triton X-100 in PBS) addition. Then, blocked in 0.5% goat serum (in PBS) for 1 hours at room temperature. The cover glasses were put in the humid chamber and specific primary antibody, incubated at 4℃ overnight. The Alexa Fluoro secondary antibodies (Life Technology) were added with 1:200 dilution and incubated at room temperature for 2 hours. Afterwards, the Hoechst dye (diluted by 1:10000 in PBS) was added and incubated for 5 minutes at room

temperature. Finally, ProLong Diamond reagent was added on the cover glasses which were put on the slide glass and sealed. The IF images were acquired by confocal microscope (Zeiss LSM510) and minimally processed by ImageJ.

In vitro dephosphorylation assay

HEK293T cells were co-transfected with the plasmids of Flag-BICD2 and Myc-Src. Then cells were lysed and collected Flag-BICD2 proteins which were phosphorylated by Src. Flag-BICD2 proteins were incubated with GST (as a control) and GST-PTPN3ΔN (residue 507-909, containing PDZ and PTP domain)-WT or GST-PTPN3ΔN-DA proteins at 37 °C for 30 minutes with in vitro PTPase buffer (25 mM Tris-HCl, pH 7.5, 2.5 mM EDTA, 5 mM DTT, 1 mM EGTA, 1 mg/ml BSA, 1 mM PMSF and protease inhibitor cocktail (Roche)). Reactions were stopped by adding sample buffer and boiling for 5 minutes. Samples were resolved by SDS-PAGE and subjected to Western blot analysis.

VSVG transport assay

Cells were transfected with GFP-VSVG for 6 hours, and treated doxycycline (10μg/ml). After transfection, cells were incubated at 40 °C for 20 hours. Then, cells were treated cycloheximide (150 ng/ml) and incubated shift to 32 °C to cause VSVG transport. After temperature shift 120 minutes, cells were fixed with 4% paraformaldehyde (in PBS) for 15 minutes, and performed immunofluorescent staining.

In addition, temperature shift 15 minutes as control.

Antibody list

Antibody name	Provider and catalog number	Concentration
Flag	Sigma-Aldrich (F1804)	1:5000 for WB 1:1000 for IF 1:1000 for IP
Phospho-tyrosine	Merk Millipore (05-321)	1:2500 for WB
HA	Santa Cruz-(sc-805)	1:5000 for WB 1:1500 for IF
Myc	Sigma- Aldrich (C3956)	1:5000 for WB
V5	Bio Rad (MCA1360)	1:5000 for WB
Src	Cell signaling (2110)	1:5000 for WB
Fyn	Cell signaling (4023s)	1:2000 for WB
α -tubulin	Sigma-Aldrich (T5168)	1:10000 for WB 1:5000 for IF
β -actin	Novus biological (NB600-501)	1:10000 for WB
GM130	BD Biosciences (610823)	1:500 for IF
EEA1	Cell signaling (3288)	1:200 for IF
TGN46	Abcam (76282)	1:200 for IF

Drosophila strains and genetics crosses

All flies were raised and crossed at 25°C.

Stoke	Genotype	Source
35405	y1 sc* v1; P{TRiP.GL00325}attP2	Bloomington
28571	y1 v1; P{TRiP.HM05057}attP2/TM3, Sb1	Bloomington
cyo/SgS-GFP;SgS3-Gal4/6B	cyo/SgS-GFP;SgS3-Gal4/6B	Generate by Jun-Kun Wen
en-GAL4>UAS-dPtpmeg/cyo	en-GAL4>UAS-dPtpmeg/cyo	Generate by Meng-Yen Li

Immunofluorescence (salivary gland of Drosophila)

The salivary glands were dissected from third instar larvae and white pupa stage, then fixed with 4% paraformaldehyde (in PBS) for 30 minutes. After washing two times with PBS, samples were perforated by 10 minutes of 0.3% PBST (Triton X-100 in PBS) and blocked 5% goat serum (in 0.3% PBST) for 1 hours after perforation. Afterwards, samples were stained with phalloidin (1:200 in 0.3% PBST) for 1 hour, then stained with Hoechst dye (1:10000 in PBS) for 10 minutes at room temperature. Finally, samples was washed two times with PBS, and mounted on the microscope slides with cover glass. The images were scanned by confocal microscope (Zeiss LSM510) and minimally processed by ImageJ.

Primers

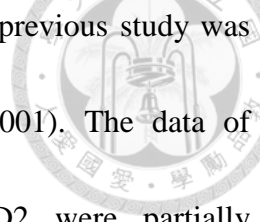| Constructs	Vector	Cutting sites	Sequences
Flag-BICD2-F	pcDNA3.1	BamHI	CTAGGGATCCATGGACTACAAGG ACGACGATGACAAGATGTCCGCG CCG
Flag-BICD2-R	pcDNA3.1	EcoRI	CTAGGAATTCTTACAGGCTCGGTG AGGC
Flag-BICD2-CC1-F	pcDNA3.1	BamHI	CTAGGGATCCATGGACTACAAGG ACGACGATGACAAGCTGGTGATG GAGGCG
Flag-BICD2-CC1-R	pcDNA3.1	EcoRI	CTAGGAATTCTTAGAAGGAATCGT TGATGCT
Flag-BICD2-CC2-F	pcDNA3.1	BamHI	CTAGGGATCCATGGACTACAAGG ACGACGATGACAAGGACCTGCTC AGTGAGCTC

Flag-BICD2-CC2-R	pcDNA3.1	EcoRI	CTAGGAATTCTTAATGGTGGTAGAGGTTGGC
Flag-BicD2-CC3-F	pcDNA3.1	BamHI	CTAGGGATCCATGGACTACAAGGACGACGATGACAAGCCTGCTGTGGACAAGGAC
Flag-BicD2-CC3-R	pcDNA3.1	EcoRI	CTAGGAATTCTTACAGGCTCGGTGAGGC
Flag-BICD2-N1-F	pcDNA3.1	BamHI	CTAGGGATCCATGGACTACAAGGACGACGATGACAAGATGTCCGCGCCG
Flag-BICD2-N1-R	pcDNA3.1	EcoRI	CTAGGAATTCTTAGAAGGAATCGTTGATGCT
Flag-BICD2-CC12-F	pcDNA3.1	BamHI	CTAGGGATCCATGGACTACAAGGACGACGATGACAAGCTGGTGATGGAGGCG
Flag-BICD2-CC12-R	pcDNA3.1	EcoRI	CTAGGAATTCTTAATGGTGGTAGAGGTTGGC
Flag-BICD2-CC23-F	pcDNA3.1	BamHI	CTAGGGATCCATGGACTACAAGGACGACGATGACAAGGACCTGCTCAGTGAGCTC
Flag-BICD2-CC23-R	pcDNA3.1	EcoRI	CTAGGAATTCTTACAGGCTCGGTGAGGC
BICD2-Y426F	pcDNA3.1		GAAGACGGTGACTTCTATGAGGTGGACATC
BICD2-Y427F	pcDNA3.1		GAAGACGGTGACTACTTTGAGGTGGACATC
BICD2-Y441F	pcDNA3.1		CTGGCCTGCAAGTTCCACGTGGCTGTGGCT
BICD2-Y476F	pcDNA3.1		GAAAAGGGCCGGTTTGAGGCTGAGGGCCAG
Flag-dBicD2-F	pcDNA3.1	EcoRI	CTAGGAATTCATGGACTACAAGGACGACGATGACAAGATGTCCAGCGCCAG
Flag-dBicD2-R	pcDNA3.1	XbaI	CTAGTCTAGATTAGAATGGATTGGCGTTACT

Results

BICD2 interacts with PTPN3 and is a substrate of PTPN3

Our previous study has shown that PTPN3 is involved in the regulation of EGFR endocytic trafficking and lung cancer cell proliferation (Li et al., 2015). However, the biological function of PTPN3 remains largely unknown. In this study, we used Mass spectrometry-based substrate trapping strategy to find the potential substrates of PTPN3. The result showed that BICD2 is one of potential substrates of PTPN3. BICD2, one of the adaptor proteins BICD family, plays an important role in intracellular transport. To confirm the data of Mass spectrometry, we first investigated the interaction between PTPN3 and BICD2 in vivo by transiently co-expressing the V5-tagged WT or substrate trapping muntant (catalytic inactive) DA form of PTPN3 (PTPN3-DA) with Flag-tagged BICD2 in HEK293T, and then the anti-V5 immunoprecipitates from cell lysates were analyzed by western blotting (Figure 1A). As shown in Fig. 1A, we found that BICD2 binds with the substrate trapping DA muntant of PTPN3 significantly. Then, we examined the direct interaction between PTPN3 and BICD2 by in vitro GST pull-down assay. Bacterially expressed Flag-BICD2 could associate with GST-PTPN3ΔN (residue 507-909, containing PDZ and PTP domain)-DA form (Figure 1B). We also observed the possibility of PTPN3 and BICD2 colocalization by immunofluorescence assay. This assay was performed in N2a cells, since neurons are extremely dependent on the
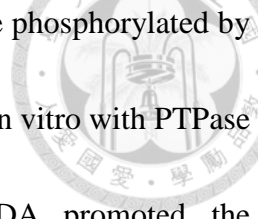
intracellular trafficking to maintain cellular function. Besides this, previous study was known that BICD2 is enriched in Golgi (Hoogenraad et al., 2001). The data of immunofluorescencet staining showed that PTPN3 and BICD2 were partially colocalized with each other (Figure 1C). Further, to determine which domains of PTPN3 are essential for binding with BICD2, we designed different truncated forms of PTPN3, including PTPN3-ΔN (delete FERM domain), PTPN3-ΔPTP (delete PTP domain), and PTPN3-PDZ (PDZ domain only) (Figure 2A). BICD2 was co-expressed with different truncated forms of PTPN3, and we found that BICD2 could interact with PTPN3-ΔN and PTPN3-ΔPTP, but not PTPN3-PDZ (Figure 2B). These results indicated that PTPN3 interacts with BICD2 in vivo and in vitro through the multiple domains binding with BICD2. Moreover, we investigated whether BICD2 is a substrate of PTPN3. BICD2 was expressed alone, and the cells were treated with sodium pervanadate, an inhibitor of protein tyrosine phosphatases, for 15 minutes prior to harvesting. BICD2 was showed to be tyrosine-phosphorylated under sodium pervanadate treatment (Figure 2C, lane 1and 2). We further confirmed PTPN3 could dephosphorylate the tyrosine-phosphorylated BICD2. PTPN3 down-regulated the phospho-tyrosine level of BICD2, and the DA form of PTPN3 could not (Figure 2C, lane 3 and lane 4). The results suggested that BICD2 is a substrate of PTPN3.

Src is the kinase of BICD2

To identify the tyrosine kinases which are likely to phosphorylate BICD2. Src, a non-receptor tyrosine kinase, has reported to act a central role in defining Golgi structure and regulating the dynamics of Golgi (Weller et al., 2010). Overexpression various mutations of BICD2 has shown to disrupt the morphology of Golgi (Neveling et al., 2013; Peeters et al., 2013). To address whether Src is the kinase of BICD2, BICD2 was co-transfected with the WT and KD (kinase dead) forms of Src. Immunoblotting data revealed that Src could phosphorylate BICD2 as seen the phospho-tyrosine band of BICD2, in contrast, the KD form of Src could not (Figure 3A). To confirm the role of Src in phosphorylating BICD2, we utilized a small molecular - dasatinib, a tyrosine kinase inhibitor of SRC family kinases and Bsr-Abl kinase. Under dasatinib treatment, the tyrosine phosphorylation level of BICD2 was reduced as compared with cells without treating dasatinib (Figure 3B). These results implicated that Src is the kinase of BICD2. To further verify the relationship between PTPN3, BICD2, and Src, we observed the level of phosphor-tyrosine in BICD2 at different groups. When co-expressed BICD2, Src and PTPN3-WT in cells, the phosphor-tyrosine level of BICD2 was decreased in comparison with group without expressing PTPN3, and the phosphor-tyrosine level of being transfected PTPN3-CS (catalytic inactive) was not reduced (Figure 3C). We also performed in vitro dephosphorylation assay. The cells
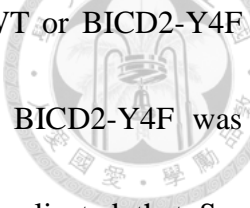
were co-expressed BICD2 and Src, then BICD2 proteins which were phosphorylated by

Src were collected and incubated with PTPN3ΔN-WT or DA forms in vitro with PTPase

buffer. We found that PTPN3ΔN-WT but not PTPN3ΔN- DA promoted the

dephosphorylation of BICD2 (Figure 3D). These results together suggested that PTPN3

and Src coordinate the tyrosine-phosphorylation of BICD2.

Src kinase phosphorylates the coiled-coil domain 2 of BICD2

To elicit the potential phosphorylation sites on BICD2 by Src, we produced different

truncated forms of BICD2, containing N1 (N-terminal and coiled-coil domain 1 (CC1)),

C12 (CC1 to CC2), C23 (CC2 to CC3), CC1 (only coiled-coil domain 1), CC2 (only

coiled-coil domain 2), CC3 (only coiled-coil domain 3) of BICD2 (Figure 4A). First, we

co-expressed BICD2-N1 or C12 or C23, and Src. BICD2-C12 and C23 but not

BICD2-N1 were phosphoorylated by Src (Figure 4B), indicating that the potential

phosphorylation sites may be between CC2 to CC3 tyrosine residues of BICD2. Further,

only coiled-coil domain 2 was phosphoorylated by Src, as co-transfected BICD2-CC1

or CC2 or CC3, and Src (Figure 4C). The coiled-coil domain 2 of BICD2 has four

tyrosine residues, Y426, Y427, Y441 and Y476. To verify which tyrosine sites are

phosphorylated by Src. WT or YF mutants, including single tyrosine mutanted and all

four tyrosine residues mutanted (Y4F), of BICD2 was expressed with Src, and only

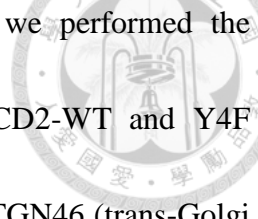BICD2-Y4F inhibited Src-induced tyrosine phosphorylation (Figure 5A). To confirm

the result, we compared the phosphor-tyrosine level that BICD2-WT or BICD2-Y4F co-expressed with Src-WT, KD. The phosphor-tyrosine level of BICD2-Y4F was significantly lower than BICD2-WT (Figure 5B). These results implicated that Src kinase phosphorylates all tyrosine residues in the coiled-coil domain 2 of BICD2.

BICD2-Y4F mutant affects the interacting level with Src but does not affect with PTPN3

To further understand whether BICD2 interacts with Src and PTPN3 depends on the phosphorylation of BICD2, co-immunoprecipitate was performed between Src and BICD2-WT or BICD2-Y4F. The level of Src binding with BICD2-Y4F mutant was significantly reduced, when compared the level of Src interacting with BICD2-WT (Figure 6A). As for PTPN3, no significant difference was observed between BICD2-WT and BICD2-Y4F associating level with PTPN3 (Figure 6B). These results indicated that the phosphorylation of BICD2 influences the interacting level with Src but not PTPN3.

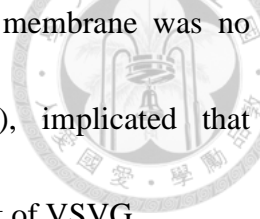## BICD2-Y4F mutant does not affect the Golgi morphology and the subcellular location

The localization of BICD2 has known that diffused the cytoplasm and specificially enriched in Golgi, ER regions and recycling endosomes (Hoogenraad et al., 2001). Some of BICD2 mutations overexpressed in cells lead to the different distribution of BICD2 and the phenomenon of fragmented Golgi (Peeters et al., 2013). To ensure the

localization of BICD2-Y4F mutant and the Golgi morphology, we performed the immunofluorescent staining with different markers. Both of BICD2-WT and Y4F mutant were strongly colocalized with GM130 (cis-Golgi marker), TGN46 (trans-Golgi marker), EEA1 (early endosome marker), and Rab11 (recycling endosome marker) (Figure 7A, B; 8A, B). And the morphology of Golgi was not significantly changed, when cells were expressed BICD2-Y4F mutant (Figure 7A, B). BICD2 mutations enhance the stability of microtubules by the increased number of acetylated long microtubule (Martinez Carrera et al., 2018), and when microtubules depolymerize will release αβ-tubulin dimers. Since this study, we initially stained α-tubulin to examine, and did not observe the difference between BICD2-WT and Y4F mutant (Figure 9).

BICD2-Y4F mutant does not have defects in the anterograde transport of VSVG

Since BICD2 regulates many aspects transport which mediated by Golgi (Martinez-Carrera and Wirth, 2015), and also acts as an adaptor protein binding with kinesin motors by coiled-coil domain 2 (Splinter et al., 2010). We investigated whether BICD2-Y4F mutant affect the anterograde transport, and examined by VSVG transport assay. The plasmid of ts045-VSVG-GFP is accumulated in the ER at 40 ℃, and then shifting to 32 ℃ transported to plasma membrane via Golgi (Yuan et al., 2014). The temperature shift 15 minutes as control, we observed GFP-VSVG was accumulated in all the control or tet-on cells of BICD2-WT and Y4F mutant (Figure 10). At 120 min

after temperature shift, the trafficking of GFP-VSVG to plasma membrane was no difference between BICD2-WT and Y4F mutant (Figure 10), implicated that BICD2-Y4F mutant does not have defect in the anterograde transport of VSVG.
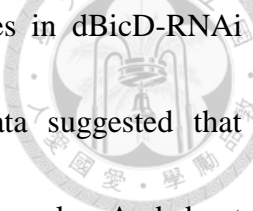
dPtpmeg and dBicD have genetic interaction, dBicD deletion rescues the wing vein loss defects caused by dPtpmeg

We also examined the genetic interaction between dPtpmeg and dBicD, since our previous study has discovered that ectopically expression of dPtpmeg in Drosophila posterior wings causes the wing vein lossing defect (Li et al., 2015). The two different dBicD-RNAi strains crossed with engrailed-dPtpmeg/Cyo, we found that dBicD-RNAi can rescue the wing vein missing phenotype induced by dPtpmeg (Figure 11)

The role of dBicD in fly salivary gland

Drosophila BicD is enriched in larval salivary glands (FlyAtlas) (http://insitu.fruitfly.org/cgi-bin/ex/insitu.pl). About the whole processes of glue granules, we roughly divided into three steps, biogenesis, transport, and degradation. To investigate whether BicD involves in the transport of glue granules, we used two dBicD-RNAi strains cross with cyo/SgS-GFP;SgS3-Gal4/6B, then dissect the salivary glands at wandering larval and white pupal stage. At wandering larval stage, the radius of gule granules in dBicD-RNAi strains were longer than control (Figure 12). And during white pupal stage, the glue granules already transport to outside and are degraded by
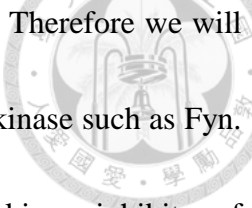
crinophagy (Csizmadia et al., 2018). The number of gule granules in dBicD-RNAi

strains were lower than control (Figure 12). These primary data suggested that

knockdown of dBicD in salivary gland affect the biogenesis of glue granules. And about

the data of white pupal stage, knockdown of dBicD maybe influence gule granules

transported to the lumen, or promote the degradation step. We will further investigate

the role of dBicD in fly salivary gland.

Discussion

PTPN3 is a well-studied non-receptor type classical PTPs in cancer. Many studies have been implicated that PTPN3 can both play the oncogenic role and tumor suppressor in different cancer cell lines, which may be dependent on tissue, species, and substrate. Moreover, our previous study has showed that PTPN3 plays a tumor suppressor by accelerating EGFR endocytic degration to inhibit the proliferation and migration in NSCLC cells and proposed a novel role of PTPN3 in endosomal sorting and endocytic trafficking (Li et al., 2015). However, the biological function of PTPN3 remains largely unknown. To further understand the role of PTPN3, we found that BICD2 is the potential substrates of PTPN3 by Mass spectrometry-based substrate trapping strategy. BICD2, a dynein adaptor protein, plays a critical role in intracellular transport. So, the aim of this study is to investigate the role of PTPN3 in intracellular transport by regulating the phosphorylation of BICD2. First, we confirmed that found BICD2 is the substrates of PTPN3. Further, we suggested that Src is a kinase of BICD2, and phosphorylates the Y426, Y427, Y441 and Y476 residues in BICD2. Since Src has reported to play an impootant role in regulating the integrity and dynamics of Golgi (Weller et al., 2010), and also some of BICD2 mutations cause the Golgi fragmentation (Neveling et al., 2013; Peeters et al., 2013). However, our immunostaining data showed that the morphology of Golgi was not changed in N2a cells overexpressed the

BICD2-Y4F mutants by two markers of Golgi, GM130 and TGN46. Therefore we will

verify BICD2 is precise phosphorylated by Src or other SRC family kinase such as Fyn.

Although we treated the dasatinib, but it is a small molecule tyrosine kinase inhibitor of

SRC family kinase and Bcr-Abl kinase, not directed against Src. We further will utilize

specific inhibitors to confirm the kinases. Also, to exclude the possibility of artifacts

from overexpression kinases, we will generate the kinases knockdown stable cell lines,

then observe the phospho-tyrosine level of BICD2 to check it.

BICD2 regulates the bidirectional transports, retrograde and anterograde transports,

by interacting with different motor proteins (Martinez-Carrera and Wirth, 2015). The

coiled-coil domain 1 of BICD2 interacts with dynein-dynactin complex to regulate

COPI-independent retrograde transport between Golgi – ER (Matanis et al., 2002). On

the other hand, BICD2 promotes the exocytosis of Rab6 exocytic vesicles (Grigoriev et

al., 2007; Schlager et al., 2010), and modulates the centrome position during mitosis

(Splinter et al., 2010) by the interaction between the coiled-coil domain 2 of BICD2 and

kinesin motor proteins. In our study, since we found out the four tyrosine site at the

coiled-coil domain 2 of BICD2, so examined whether BICD2-Y4F mutant affect the

anterograde transport by VSVG transport assay. But the result indicated that the mutant

does not have defects in the anterograde transport of VSVG. We will do more times to

confirm the results, and also generate the phospho-mimicking mutant of BICD2 to do

the experiments. Various BICD2 mutations affect the interaction with its binding proteins (Oates et al., 2013), and further we can investigate this aspect.
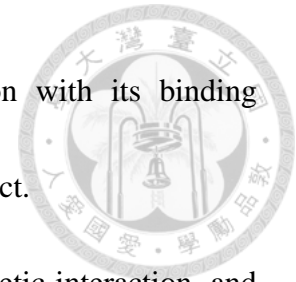
In *Drosophila*, we discovered that dPtpmeg and dBicD have genetic interaction, and dBicD could rescue the wing vein loss defects caused by dPtpmeg. Further, we will check the interaction between dPtpmeg and dBicD by immunoprecipitation and western blotting. Moreover, the expression level of *Drosophila* BicD is high in larval salivary glands (FlyAtlas) (http://insitu.fruitfly.org/cgi-bin/ex/insitu.pl). At larval stage, the salivary glands synthesis glue granules, containing highly glycosylated glue proteins (Beckendorf and Kafatos, 1976; Korge, 1977), which is transported through the ER and Golgi before forming regulated secretory granules at the TGN (Burgess et al., 2011; Thomopoulos and Kastritsis, 1979). Then, the mature glue granules are secreted to the salivary gland lumen and transported to outside for pupa adhering (Biyasheva et al., 2001; Korge, 1977). After secretion, the granules are degradged by crinophagy, a secretory granule-specific autophagic process (Csizmadia et al., 2018; Harrod and Kastritsis, 1972). We investigated whether *Drosophila* BicD involves in the transport of glue granules, and observed two stages of larva. The result suggested that dBicD may be involve in the biogenesis of glue granules. To more efficiently verify the role of dBicD in the whole glue granules processes, we will use FLP-FRT system.

References

Akhmanova, A., and Hammer, J.A., 3rd (2010). Linking molecular motors to membrane cargo. Curr Opin Cell Biol *22*, 479-487.

Alonso, A., Sasin, J., Bottini, N., Friedberg, I., Friedberg, I., Osterman, A., Godzik, A., Hunter, T., Dixon, J., and Mustelin, T. (2004). Protein tyrosine phosphatases in the human genome. Cell *117*, 699-711.

Andersen, J.N., Jansen, P.G., Echwald, S.M., Mortensen, O.H., Fukada, T., Del Vecchio, R., Tonks, N.K., and Moller, N.P. (2004). A genomic perspective on protein tyrosine phosphatases: gene structure, pseudogenes, and genetic disease linkage. FASEB J *18*, 8-30.

Angers-Loustau, A., Cote, J.F., and Tremblay, M.L. (1999). Roles of protein tyrosine phosphatases in cell migration and adhesion. Biochem Cell Biol *77*, 493-505.

Beckendorf, S.K., and Kafatos, F.C. (1976). Differentiation in the salivary glands of Drosophila melanogaster: characterization of the glue proteins and their developmental appearance. Cell *9*, 365-373.

Beltran, P.J., and Bixby, J.L. (2003). Receptor protein tyrosine phosphatases as mediators of cellular adhesion. Front Biosci *8*, d87-99.

Biyasheva, A., Do, T.V., Lu, Y., Vaskova, M., and Andres, A.J. (2001). Glue secretion in the Drosophila salivary gland: a model for steroid-regulated exocytosis. Dev Biol *231*, 234-251.

Bretscher, A., Edwards, K., and Fehon, R.G. (2002). ERM proteins and merlin: integrators at the cell cortex. Nat Rev Mol Cell Biol *3*, 586-599.

Bruccoleri, R.E., Novotny, J., Keck, P., and Cohen, C. (1986). Two-stranded alpha-helical coiled-coils of fibrous proteins: theoretical analysis of supercoil formation. Biophys J *49*, 79-81.

Bullock, S.L., and Ish-Horowicz, D. (2001). Conserved signals and machinery for RNA transport in Drosophila oogenesis and embryogenesis. Nature *414*, 611-616.

Burgess, J., Jauregui, M., Tan, J., Rollins, J., Lallet, S., Leventis, P.A., Boulianne, G.L., Chang, H.C., Le Borgne, R., Kramer, H.*, et al.* (2011). AP-1 and clathrin are essential for secretory granule biogenesis in Drosophila. Mol Biol Cell *22*, 2094-2105.

Chase, K., Carrier, D.R., Adler, F.R., Ostrander, E.A., and Lark, K.G. (2005). Interaction between the X chromosome and an autosome regulates size sexual dimorphism in Portuguese Water Dogs. Genome Res *15*, 1820-1824.

Cheng, A., Dube, N., Gu, F., and Tremblay, M.L. (2002). Coordinated action of protein tyrosine phosphatases in insulin signal transduction. Eur J Biochem *269*, 1050-1059.

Chishti, A.H., Kim, A.C., Marfatia, S.M., Lutchman, M., Hanspal, M., Jindal, H., Liu, S.C., Low, P.S., Rouleau, G.A., Mohandas, N.*, et al.* (1998). The FERM domain: a

unique module involved in the linkage of cytoplasmic proteins to the membrane. Trends Biochem Sci *23*, 281-282.

Csizmadia, T., Lorincz, P., Hegedus, K., Szeplaki, S., Low, P., and Juhasz, G. (2018). Molecular mechanisms of developmentally programmed crinophagy in Drosophila. J Cell Biol *217*, 361-374.

Dharan, A., Opp, S., Abdel-Rahim, O., Keceli, S.K., Imam, S., Diaz-Griffero, F., and Campbell, E.M. (2017). Bicaudal D2 facilitates the cytoplasmic trafficking and nuclear import of HIV-1 genomes during infection. Proc Natl Acad Sci U S A *114*, E10707-E10716.

Edwards, K., Davis, T., Marcey, D., Kurihara, J., and Yamamoto, D. (2001). Comparative analysis of the Band 4.1/ezrin-related protein tyrosine phosphatase Pez from two Drosophila species: implications for structure and function. Gene *275*, 195-205.

Fu, M.M., and Holzbaur, E.L. (2013). JIP1 regulates the directionality of APP axonal transport by coordinating kinesin and dynein motors. J Cell Biol *202*, 495-508.

Gao, Q., Zhao, Y.J., Wang, X.Y., Guo, W.J., Gao, S., Wei, L., Shi, J.Y., Shi, G.M., Wang, Z.C., Zhang, Y.N.*, et al.* (2014). Activating mutations in PTPN3 promote cholangiocarcinoma cell proliferation and migration and are associated with tumor recurrence in patients. Gastroenterology *146*, 1397-1407.

Garton, A.J., Burnham, M.R., Bouton, A.H., and Tonks, N.K. (1997). Association of PTP-PEST with the SH3 domain of p130cas; a novel mechanism of protein tyrosine phosphatase substrate recognition. Oncogene *15*, 877-885.

Grigoriev, I., Splinter, D., Keijzer, N., Wulf, P.S., Demmers, J., Ohtsuka, T., Modesti, M., Maly, I.V., Grosveld, F., Hoogenraad, C.C.*, et al.* (2007). Rab6 regulates transport and targeting of exocytotic carriers. Dev Cell *13*, 305-314.

Han, S., Williams, S., and Mustelin, T. (2000). Cytoskeletal protein tyrosine phosphatase PTPH1 reduces T cell antigen receptor signaling. Eur J Immunol *30*, 1318-1325.

Hancock, W.O. (2014). Bidirectional cargo transport: moving beyond tug of war. Nat Rev Mol Cell Biol *15*, 615-628.

Harrod, M.J., and Kastritsis, C.D. (1972). Developmental studies in Drosophila. II. Ultrastructural analysis of the salivary glands of Drosophila pseudoobscura during some stages of development. J Ultrastruct Res *38*, 482-499.

Hendriks, W.J., Elson, A., Harroch, S., Pulido, R., Stoker, A., and den Hertog, J. (2013). Protein tyrosine phosphatases in health and disease. FEBS J *280*, 708-730.

Hirokawa, N. (1998). Kinesin and dynein superfamily proteins and the mechanism of organelle transport. Science *279*, 519-526.

Hoogenraad, C.C., Akhmanova, A., Howell, S.A., Dortland, B.R., De Zeeuw, C.I., Willemsen, R., Visser, P., Grosveld, F., and Galjart, N. (2001). Mammalian

Golgi-associated Bicaudal-D2 functions in the dynein-dynactin pathway by interacting with these complexes. EMBO J *20*, 4041-4054.

Hoogenraad, C.C., Wulf, P., Schiefermeier, N., Stepanova, T., Galjart, N., Small, J.V., Grosveld, F., de Zeeuw, C.I., and Akhmanova, A. (2003). Bicaudal D induces selective dynein-mediated microtubule minus end-directed transport. EMBO J *22*, 6004-6015.

Hou, S.W., Zhi, H.Y., Pohl, N., Loesch, M., Qi, X.M., Li, R.S., Basir, Z., and Chen, G. (2010). PTPH1 dephosphorylates and cooperates with p38gamma MAPK to increase ras oncogenesis through PDZ-mediated interaction. Cancer Res *70*, 2901-2910.

Houalla, T., Hien Vuong, D., Ruan, W., Suter, B., and Rao, Y. (2005). The Ste20-like kinase misshapen functions together with Bicaudal-D and dynein in driving nuclear migration in the developing drosophila eye. Mech Dev *122*, 97-108.

Hung, A.Y., and Sheng, M. (2002). PDZ domains: structural modules for protein complex assembly. J Biol Chem *277*, 5699-5702.

Huynh, W., and Vale, R.D. (2017). Disease-associated mutations in human BICD2 hyperactivate motility of dynein-dynactin. J Cell Biol *216*, 3051-3060.

Jaarsma, D., van den Berg, R., Wulf, P.S., van Erp, S., Keijzer, N., Schlager, M.A., de Graaff, E., De Zeeuw, C.I., Pasterkamp, R.J., Akhmanova, A*., et al.* (2014). A role for Bicaudal-D2 in radial cerebellar granule cell migration. Nat Commun *5*, 3411.

Januschke, J., Nicolas, E., Compagnon, J., Formstecher, E., Goud, B., and Guichet, A. (2007). Rab6 and the secretory pathway affect oocyte polarity in Drosophila. Development *134*, 3419-3425.

Jung, Y., Kim, P., Jung, Y., Keum, J., Kim, S.N., Choi, Y.S., Do, I.G., Lee, J., Choi, S.J., Kim, S*., et al.* (2012). Discovery of ALK-PTPN3 gene fusion from human non-small cell lung carcinoma cell line using next generation RNA sequencing. Genes Chromosomes Cancer *51*, 590-597.

Karki, S., and Holzbaur, E.L. (1999). Cytoplasmic dynein and dynactin in cell division and intracellular transport. Curr Opin Cell Biol *11*, 45-53.
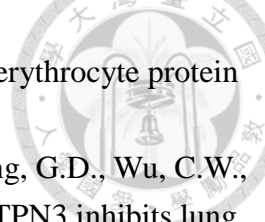
Katagiri, T., Ogimoto, M., Hasegawa, K., Arimura, Y., Mitomo, K., Okada, M., Clark, M.R., Mizuno, K., and Yakura, H. (1999). CD45 negatively regulates lyn activity by dephosphorylating both positive and negative regulatory tyrosine residues in immature B cells. J Immunol *163*, 1321-1326.
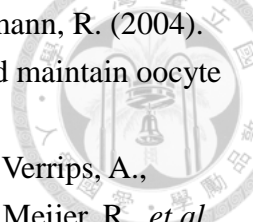
Kim, E., and Sheng, M. (2004). PDZ domain proteins of synapses. Nat Rev Neurosci *5*, 771-781.
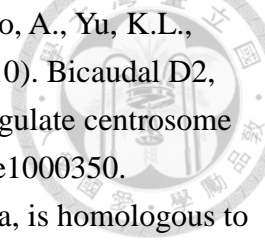
Korge, G. (1977). Larval saliva in Drosophila melanogaster: production, composition, and relationship to chromosome puffs. Dev Biol *58*, 339-355.

Larsen, K.S., Xu, J., Cermelli, S., Shu, Z., and Gross, S.P. (2008). BicaudalD actively regulates microtubule motor activity in lipid droplet transport. PLoS One *3*, e3763.

Lee, J.M., Fournel, M., Veillette, A., and Branton, P.E. (1996). Association of CD45 with Lck and components of the Ras signalling pathway in pervanadate-treated mouse

T-cell lines. Oncogene *12*, 253-263.

Leto, T.L., and Marchesi, V.T. (1984). A structural model of human erythrocyte protein 4.1. J Biol Chem *259*, 4603-4608.

Li, M.Y., Lai, P.L., Chou, Y.T., Chi, A.P., Mi, Y.Z., Khoo, K.H., Chang, G.D., Wu, C.W., Meng, T.C., and Chen, G.C. (2015). Protein tyrosine phosphatase PTPN3 inhibits lung cancer cell proliferation and migration by promoting EGFR endocytic degradation. Oncogene *34*, 3791-3803.

Liu, F., Sells, M.A., and Chernoff, J. (1998). Protein tyrosine phosphatase 1B negatively regulates integrin signaling. Curr Biol *8*, 173-176.

Liu, Y., Salter, H.K., Holding, A.N., Johnson, C.M., Stephens, E., Lukavsky, P.J., Walshaw, J., and Bullock, S.L. (2013). Bicaudal-D uses a parallel, homodimeric coiled coil with heterotypic registry to coordinate recruitment of cargos to dynein. Genes Dev *27*, 1233-1246.

Mach, J.M., and Lehmann, R. (1997). An Egalitarian-BicaudalD complex is essential for oocyte specification and axis determination in Drosophila. Genes Dev *11*, 423-435.

Maehama, T., and Dixon, J.E. (1998). The tumor suppressor, PTEN/MMAC1, dephosphorylates the lipid second messenger, phosphatidylinositol 3,4,5-trisphosphate. J Biol Chem *273*, 13375-13378.

Martinez-Carrera, L.A., and Wirth, B. (2015). Dominant spinal muscular atrophy is caused by mutations in BICD2, an important golgin protein. Front Neurosci *9*, 401.

Martinez Carrera, L.A., Gabriel, E., Donohoe, C.D., Holker, I., Mariappan, A., Storbeck, M., Uhlirova, M., Gopalakrishnan, J., and Wirth, B. (2018). Novel insights into SMALED2: BICD2 mutations increase microtubule stability and cause defects in axonal and NMJ development. Hum Mol Genet *27*, 1772-1784.

Matanis, T., Akhmanova, A., Wulf, P., Del Nery, E., Weide, T., Stepanova, T., Galjart, N., Grosveld, F., Goud, B., De Zeeuw, C.I.*, et al.* (2002). Bicaudal-D regulates COPI-independent Golgi-ER transport by recruiting the dynein-dynactin motor complex. Nat Cell Biol *4*, 986-992.

McKenney, R.J., Huynh, W., Tanenbaum, M.E., Bhabha, G., and Vale, R.D. (2014). Activation of cytoplasmic dynein motility by dynactin-cargo adapter complexes. Science *345*, 337-341.

McKenney, R.J., Huynh, W., Vale, R.D., and Sirajuddin, M. (2016). Tyrosination of alpha-tubulin controls the initiation of processive dynein-dynactin motility. EMBO J *35*, 1175-1185.

Mohler, J., and Wieschaus, E.F. (1986). Dominant maternal-effect mutations of Drosophila melanogaster causing the production of double-abdomen embryos. Genetics *112*, 803-822.

Motiwala, T., and Jacob, S.T. (2006). Role of Protein Tyrosine Phosphatases in Cancer. *81*, 297-329.

Navarro, C., Puthalakath, H., Adams, J.M., Strasser, A., and Lehmann, R. (2004). Egalitarian binds dynein light chain to establish oocyte polarity and maintain oocyte fate. Nat Cell Biol *6*, 427-435.

Neveling, K., Martinez-Carrera, L.A., Holker, I., Heister, A., Verrips, A., Hosseini-Barkooie, S.M., Gilissen, C., Vermeer, S., Pennings, M., Meijer, R.*, et al.* (2013). Mutations in BICD2, which encodes a golgin and important motor adaptor, cause congenital autosomal-dominant spinal muscular atrophy. Am J Hum Genet *92*, 946-954.

Oates, E.C., Rossor, A.M., Hafezparast, M., Gonzalez, M., Speziani, F., MacArthur, D.G., Lek, M., Cottenie, E., Scoto, M., Foley, A.R.*, et al.* (2013). Mutations in BICD2 cause dominant congenital spinal muscular atrophy and hereditary spastic paraplegia. Am J Hum Genet *92*, 965-973.

Ostman, A., and Bohmer, F.D. (2001). Regulation of receptor tyrosine kinase signaling by protein tyrosine phosphatases. Trends Cell Biol *11*, 258-266.

Peeters, K., Litvinenko, I., Asselbergh, B., Almeida-Souza, L., Chamova, T., Geuens, T., Ydens, E., Zimon, M., Irobi, J., De Vriendt, E.*, et al.* (2013). Molecular defects in the motor adaptor BICD2 cause proximal spinal muscular atrophy with autosomal-dominant inheritance. Am J Hum Genet *92*, 955-964.

Pilecka, I., Patrignani, C., Pescini, R., Curchod, M.L., Perrin, D., Xue, Y., Yasenchak, J., Clark, A., Magnone, M.C., Zaratin, P.*, et al.* (2007). Protein-tyrosine phosphatase H1 controls growth hormone receptor signaling and systemic growth. J Biol Chem *282*, 35405-35415.

Ran, B., Bopp, R., and Suter, B. (1994). Null alleles reveal novel requirements for Bic-D during Drosophila oogenesis and zygotic development. Development *120*, 1233-1242.

Rheinlander, A., Schraven, B., and Bommhardt, U. (2018). CD45 in human physiology and clinical medicine. Immunol Lett *196*, 22-32.

Schlager, M.A., Hoang, H.T., Urnavicius, L., Bullock, S.L., and Carter, A.P. (2014). In vitro reconstitution of a highly processive recombinant human dynein complex. EMBO J *33*, 1855-1868.

Schlager, M.A., and Hoogenraad, C.C. (2009). Basic mechanisms for recognition and transport of synaptic cargos. Mol Brain *2*, 25.

Schlager, M.A., Kapitein, L.C., Grigoriev, I., Burzynski, G.M., Wulf, P.S., Keijzer, N., de Graaff, E., Fukuda, M., Shepherd, I.T., Akhmanova, A.*, et al.* (2010). Pericentrosomal targeting of Rab6 secretory vesicles by Bicaudal-D-related protein 1 (BICDR-1) regulates neuritogenesis. EMBO J *29*, 1637-1651.

Schupbach, T., and Wieschaus, E. (1991). Female sterile mutations on the second chromosome of Drosophila melanogaster. II. Mutations blocking oogenesis or altering egg morphology. Genetics *129*, 1119-1136.

Splinter, D., Tanenbaum, M.E., Lindqvist, A., Jaarsma, D., Flotho, A., Yu, K.L., Grigoriev, I., Engelsma, D., Haasdijk, E.D., Keijzer, N.*, et al.* (2010). Bicaudal D2, dynein, and kinesin-1 associate with nuclear pore complexes and regulate centrosome and nuclear positioning during mitotic entry. PLoS Biol *8*, e1000350.

Steward, R. (1987). Dorsal, an embryonic polarity gene in Drosophila, is homologous to the vertebrate proto-oncogene, c-rel. Science *238*, 692-694.

Swan, A., Nguyen, T., and Suter, B. (1999). Drosophila Lissencephaly-1 functions with Bic-D and dynein in oocyte determination and nuclear positioning. Nat Cell Biol *1*, 444-449.

Swan, A., and Suter, B. (1996). Role of Bicaudal-D in patterning the Drosophila egg chamber in mid-oogenesis. Development *122*, 3577-3586.

Terenzio, M., and Schiavo, G. (2010). The more, the better: the BICD family gets bigger. EMBO J *29*, 1625-1626.

Thomopoulos, G.N., and Kastritsis, C.D. (1979). A comparative ultrastructural study of 'glue' production and secretion of the salivary glands in different species of theDrosophila melanogaster group. Wilehm Roux Arch Dev Biol *187*, 329-354.

Titus, M.A. (2018). Myosin-Driven Intracellular Transport. Cold Spring Harb Perspect Biol *10*.

Tonks, N.K. (2006). Protein tyrosine phosphatases: from genes, to function, to disease. Nat Rev Mol Cell Biol *7*, 833-846.

Vale, R.D. (2003). The molecular motor toolbox for intracellular transport. Cell *112*, 467-480.

van Spronsen, M., Mikhaylova, M., Lipka, J., Schlager, M.A., van den Heuvel, D.J., Kuijpers, M., Wulf, P.S., Keijzer, N., Demmers, J., Kapitein, L.C.*, et al.* (2013). TRAK/Milton motor-adaptor proteins steer mitochondrial trafficking to axons and dendrites. Neuron *77*, 485-502.

Vazquez-Pianzola, P., Adam, J., Haldemann, D., Hain, D., Urlaub, H., and Suter, B. (2014). Clathrin heavy chain plays multiple roles in polarizing the Drosophila oocyte downstream of Bic-D. Development *141*, 1915-1926.

Wadham, C., Gamble, J.R., Vadas, M.A., and Khew-Goodall, Y. (2000). Translocation of protein tyrosine phosphatase Pez/PTPD2/PTP36 to the nucleus is associated with induction of cell proliferation. J Cell Sci *113 (Pt 17)*, 3117-3123.

Weller, S.G., Capitani, M., Cao, H., Micaroni, M., Luini, A., Sallese, M., and McNiven, M.A. (2010). Src kinase regulates the integrity and function of the Golgi apparatus via activation of dynamin 2. Proc Natl Acad Sci U S A *107*, 5863-5868.

Welte, M.A. (2004). Bidirectional transport along microtubules. Curr Biol *14*, R525-537.

Wharton, R.P., and Struhl, G. (1989). Structure of the Drosophila BicaudalD protein and its role in localizing the the posterior determinant nanos. Cell *59*, 881-892.

Whited, J.L., Robichaux, M.B., Yang, J.C., and Garrity, P.A. (2007). Ptpmeg is required for the proper establishment and maintenance of axon projections in the central brain of Drosophila. Development *134*, 43-53.

Yamada, K.M., and Araki, M. (2001). Tumor suppressor PTEN: modulator of cell signaling, growth, migration and apoptosis. J Cell Sci *114*, 2375-2382.

Yuan, W.C., Lee, Y.R., Lin, S.Y., Chang, L.Y., Tan, Y.P., Hung, C.C., Kuo, J.C., Liu, C.H., Lin, M.Y., Xu, M.*, et al.* (2014). K33-Linked Polyubiquitination of Coronin 7 by Cul3-KLHL20 Ubiquitin E3 Ligase Regulates Protein Trafficking. Mol Cell *54*, 586-600.

Zhang, S.H., Kobayashi, R., Graves, P.R., Piwnica-Worms, H., and Tonks, N.K. (1997). Serine phosphorylation-dependent association of the band 4.1-related protein-tyrosine phosphatase PTPH1 with 14-3-3beta protein. J Biol Chem *272*, 27281-27287.

Zhang, S.H., Liu, J., Kobayashi, R., and Tonks, N.K. (1999). Identification of the cell cycle regulator VCP (p97/CDC48) as a substrate of the band 4.1-related protein-tyrosine phosphatase PTPH1. J Biol Chem *274*, 17806-17812.

Figures

A.

B.

(By Jhen-jia Fan)
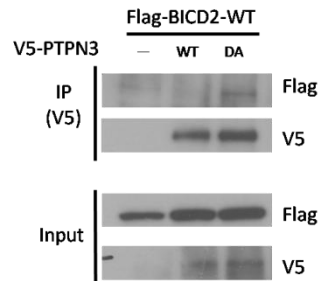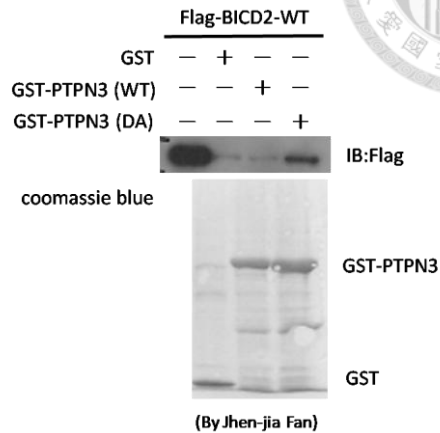
C.
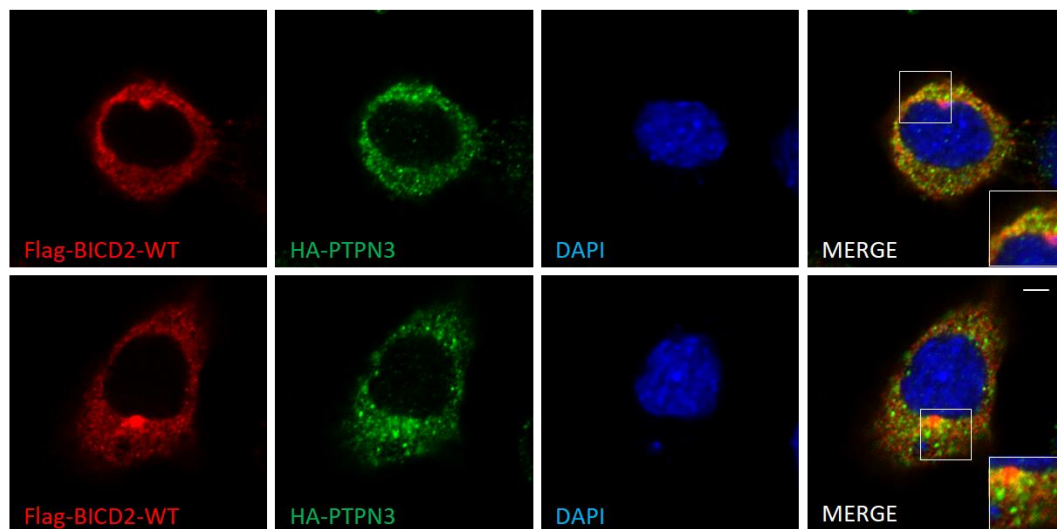
Figure 1. BICD2 interacts with PTPN3 in vivo and in vitro

(A) HEK293T cells were transiently cotransfected Flag-BICD2 with V5-PTPN3-WT or V5-PTPN3-DA. After 24 hours transfection, whole cell lysates were immunoprecipitated with anti-V5 antibody and analyzed by western blotting with indicated antibodies.

(B) Bacterially expressed Flag-BICD2 was incubated with the equal amounts of GST only, GST-PTPN3ΔN-WT or GST-PTPN3ΔN-DA proteins for in vitro GST pull-down assays.

(C) N2a cells were transiently transfected with Flag-BICD2 and HA-PTPN3. After transfection 24 hours, cells were immunostained with anti-Flag (red) and anti-HA (green) antibodies. Nuclei were stained by DAPI (blue). Scale bar:3 μm.
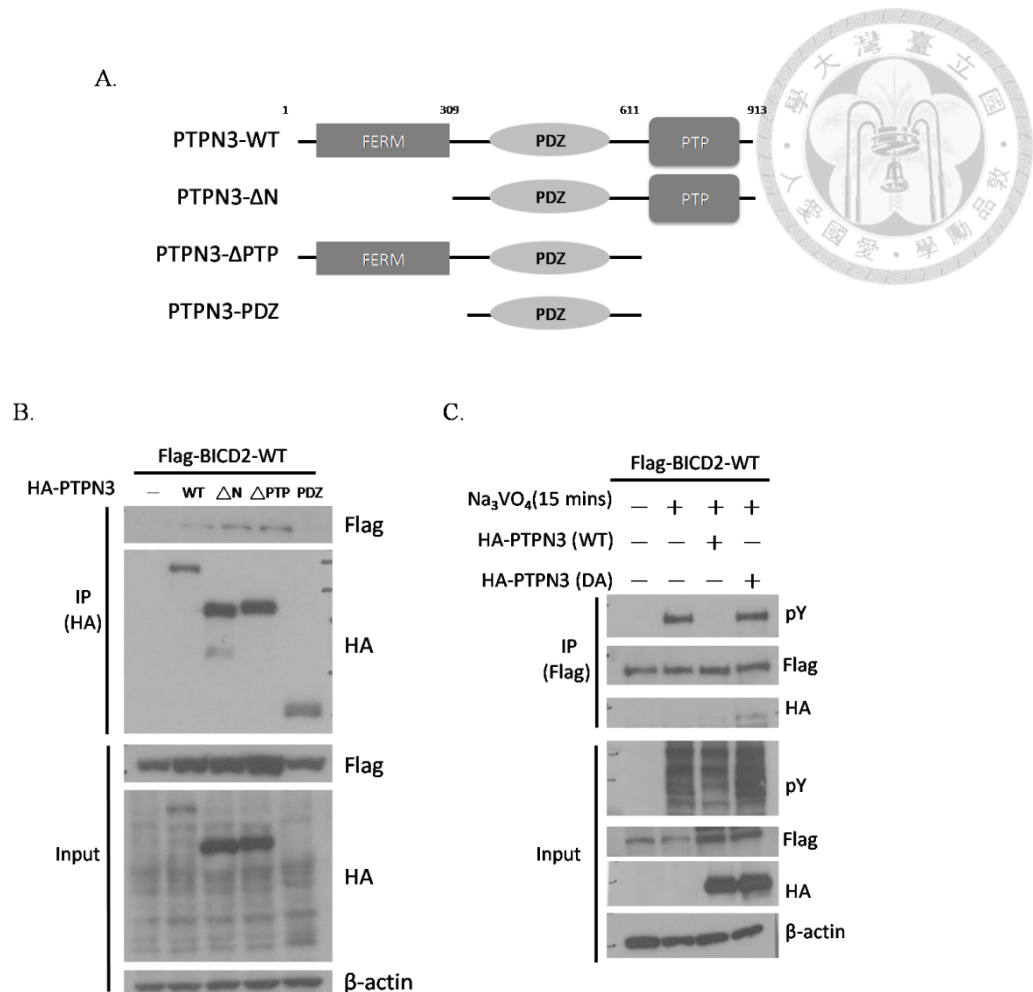
Figure 2. PTPN3 interacts with BICD2 through the multiple domains, and BICD2 is a substrate of PTPN3

(A) The domain architecture of PTPN3, including FERM, PDZ and PTP domains. PTPN3-ΔN (FERM domain deletion mutant), PTPN3-ΔPTP (PTP domain deletion mutant), and PTPN3-PDZ (PDZ domain only) are different truncated forms of PTPN3.

(B) HEK293T cells were transiently cotransfected Flag-BICD2 with wild type HA-PTPN3 or different truncated forms of PTPN3, ΔN, ΔPTP, PDZ only for 24 hours. Whole cell lysates were immunoprecipitated with anti-HA antibody and analyzed by western blotting with indicated antibodies.

(C) HEK293T cells were transiently cotransfected Flag-BICD2 with wild type HA-PTPN3 or DA mutant for 24 hours. Prior to harvesting cells were treated with 0.1mM sodium pervanadate for 15 minutes. Whole cell lysates were immunoprecipitated with anti-Flag antibody and analyzed by western blotting with antibodies as indicated.
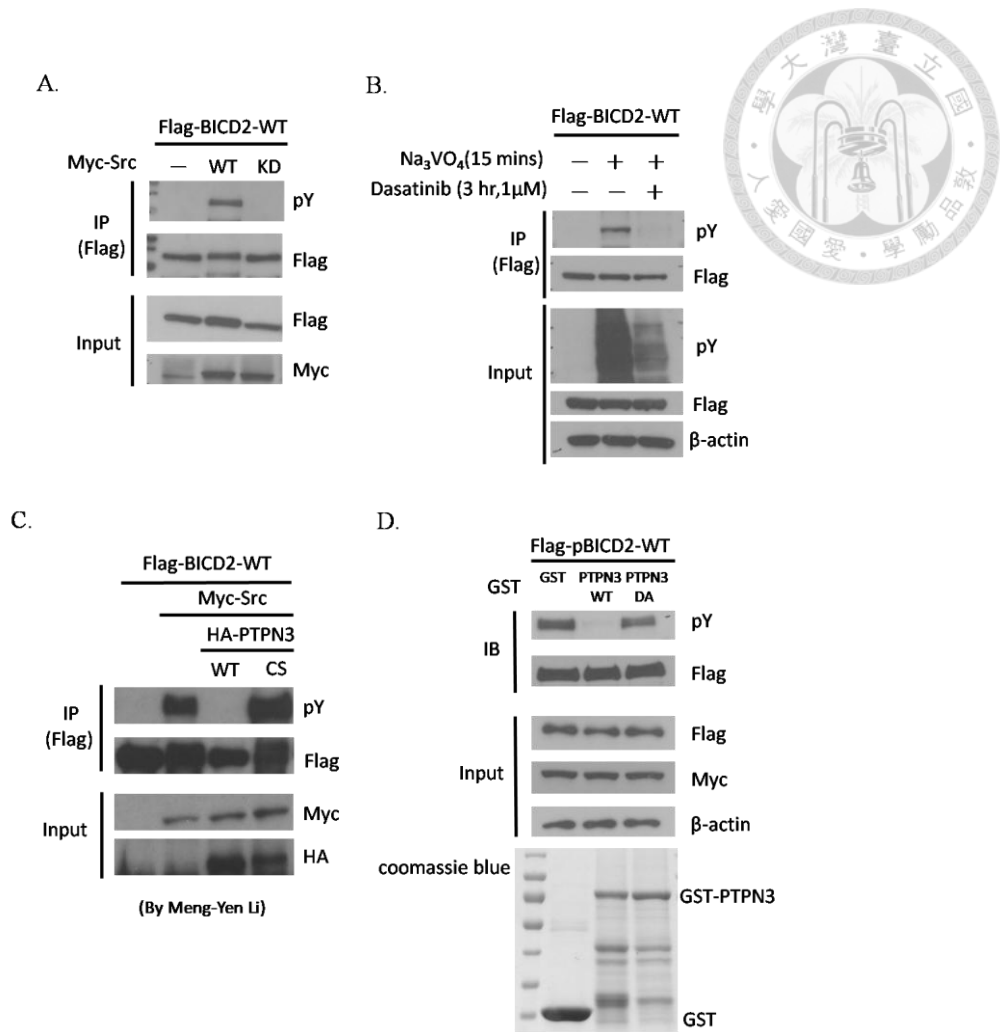
Figure 3. Src is the kinase of BICD2

(A) HEK293T cells were transiently cotransfected Flag-BICD2 with Myc-Src-WT or Myc-Src-KD (kinase-dead). After 24 hours transfection, whole cell lysates were immunoprecipitated with anti-Flag antibody and analyzed by western blotting with indicated antibodies.

(B) HEK293T cells were transiently transfected Flag-BICD2 for 24 hours. After transfection, cells were incubated in fresh medium with or without 1μM dasatinib for 3 hours. Prior to harvesting cells were treated with 0.1mM sodium pervanadate for 15 minutes. Whole cell lysates were immunoprecipitated with anti-Flag antibody and analyzed by western blotting with antibodies as indicated.

(C) HEK293T cells were transiently cotransfected Flag-BICD2 with Myc-Src, wild type HA-PTPN3 or CS mutant (catalytic inactive). After 24 hours transfection, whole cell lysates were immunoprecipitated with anti-Flag antibody and analyzed by western blotting with indicated antibodies.

(D) PTPN3 dephosphorylates Flag-BICD2 *in vitro.* Equal amounts of GST only, GST-PTPN3ΔN-WT or GST-PTPN3ΔN-DA proteins were co-incubated with Flag-BICD2 proteins which were phosphorylated by Src in the PTPase buffer at 37°C for 30 minutes.
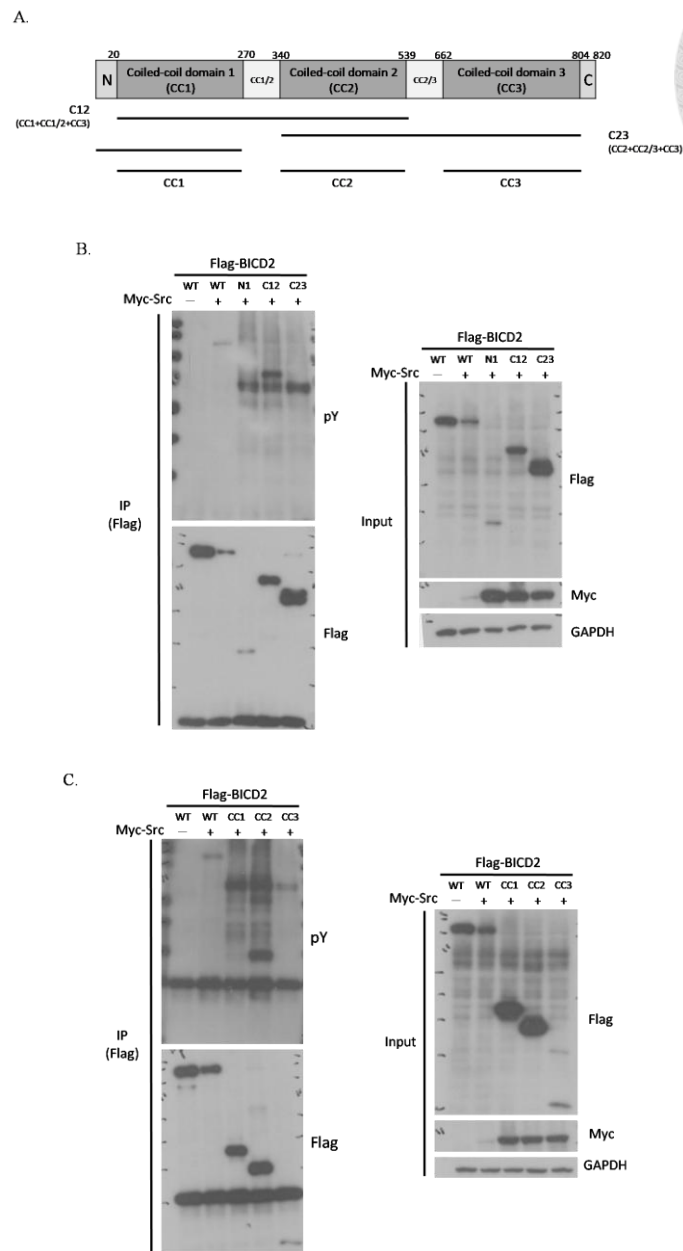
Figure 4. Src kinase phosphorylates the coiled-coil domain 2 of BICD2

(A) The domain architecture of BICD2. N1 (N-terminal and coiled-coil domain 1 (CC1)), C12 (CC1 to CC2), C23 (CC2 to CC3), CC1 (only coiled-coil domain 1), CC2 (only coiled-coil domain 2), and CC3 (only coiled-coil domain 3).
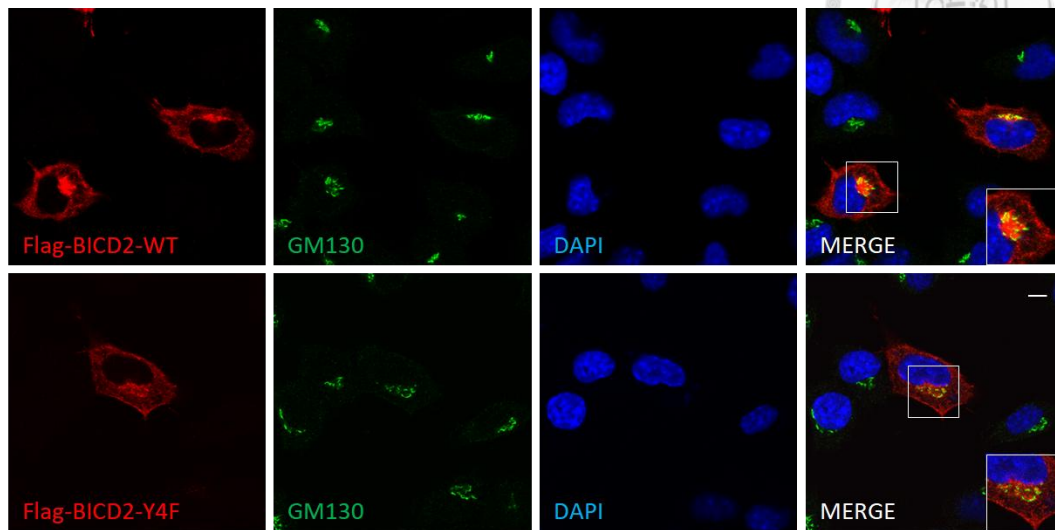
(B) HEK293T cells were transiently cotransfected Flag-BICD2-WT, N1, C12, or C23 with Myc-Src. After 24 hours transfection, whole cell lysates were immunoprecipitated with anti-Flag antibody and analyzed by western blotting with indicated antibodies.

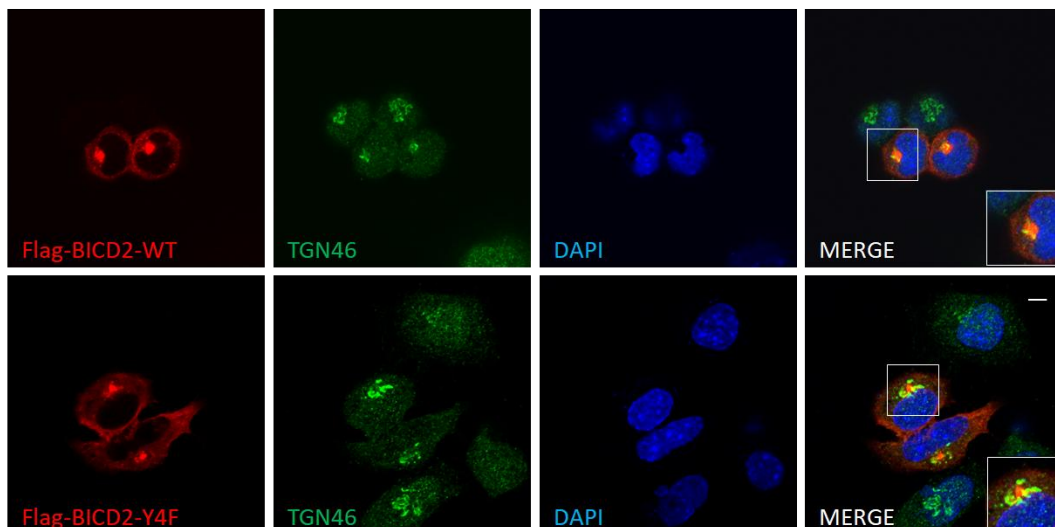(C) HEK293T cells were transiently cotransfected Flag-BICD2-WT, CC1, CC2, or CC3 with Myc-Src. After 24 hours transfection, whole cell lysates were immunoprecipitated with anti-Flag antibody and analyzed by western blotting with antibodies as indicated.

A.

B.
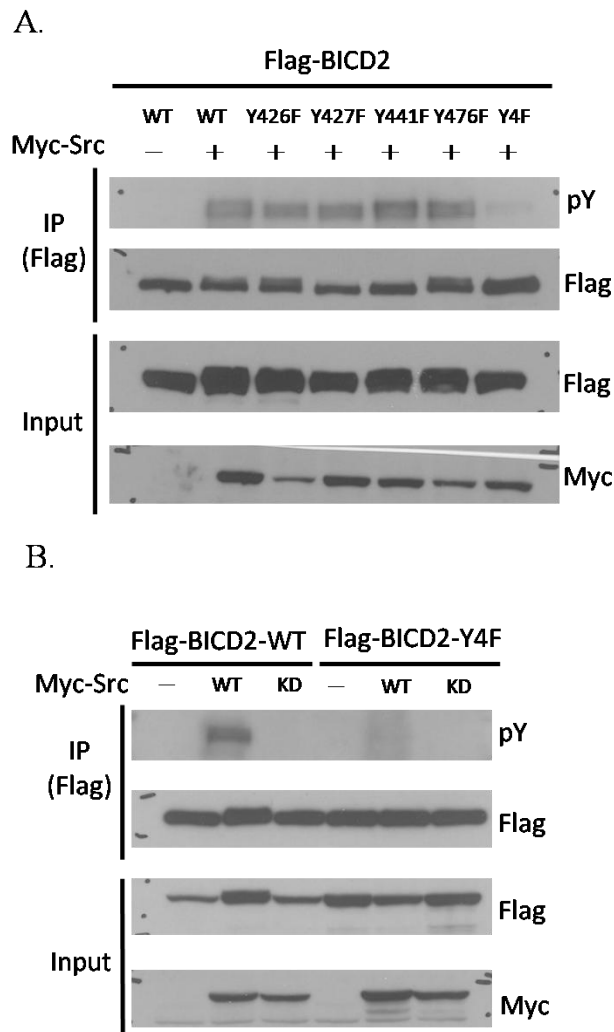
Figure 5. Src kinase phosphorylates four tyrosine residues in the coiled-coil domain 2 of BICD2

(A) HEK293T cells were transiently cotransfected Flag-BICD2-WT, Y426F, Y427F, Y441F, Y476F, or Y4F with Myc-Src. After 24 hours transfection, whole cell lysates were immunoprecipitated with anti-Flag antibody and analyzed by western blotting with antibodies as indicated.

(B) HEK293T cells were transiently cotransfected Flag-BICD2-WT or Flag-BICD2-Y4F with Myc-Src-WT or KD forms for 24 hours. After transfection, whole cell lysates were immunoprecipitated with anti-Flag antibody and analyzed by western blotting with indicated antibodies.

A.

B.
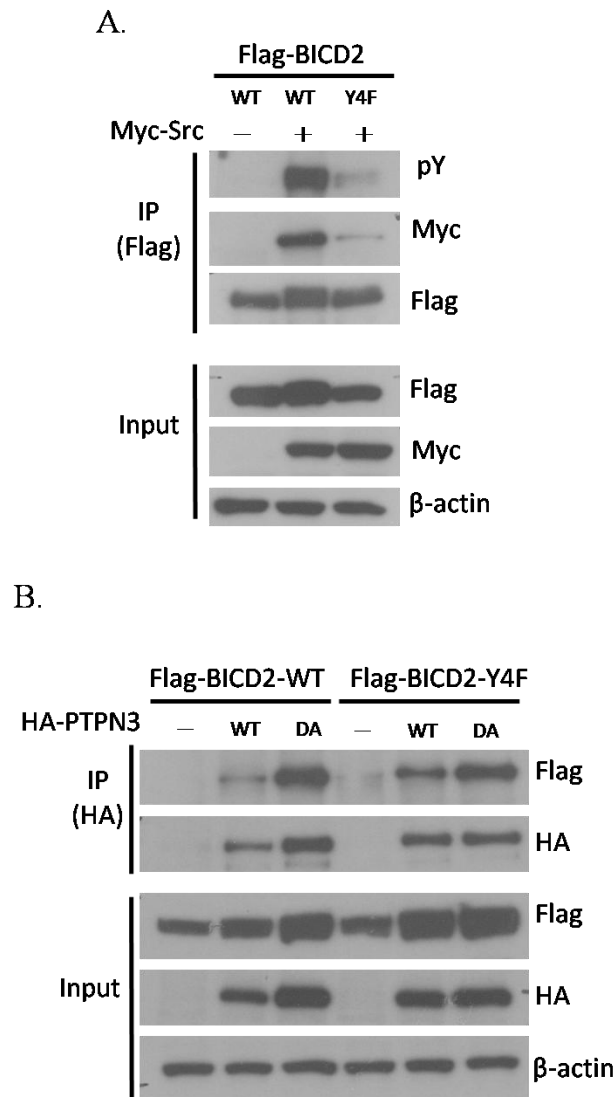
Figure 6. BICD2-Y4F mutant affects the interacting level with Src but does not affect with PTPN3

(A) HEK293T cells were transiently cotransfected Flag-BICD2-WT or Flag-BICD2-Y4F with Myc-Src-WT for 24 hours. After transfection, whole cell lysates were immunoprecipitated with anti-Flag antibody and analyzed by western blotting with indicated antibodies.

(B) HEK293T cells were transiently cotransfected Flag-BICD2-WT or Flag-BICD2-Y4F with HA-PTPN3 or DA mutant for 24 hours. After transfection, whole cell lysates were immunoprecipitated with anti-HA antibody and analyzed by western blotting with indicated antibodies.

A.

B.

Figure 7. BICD2-Y4F mutant does not affect the Golgi morphology and the subcellular location

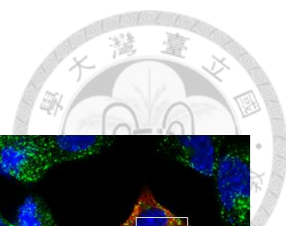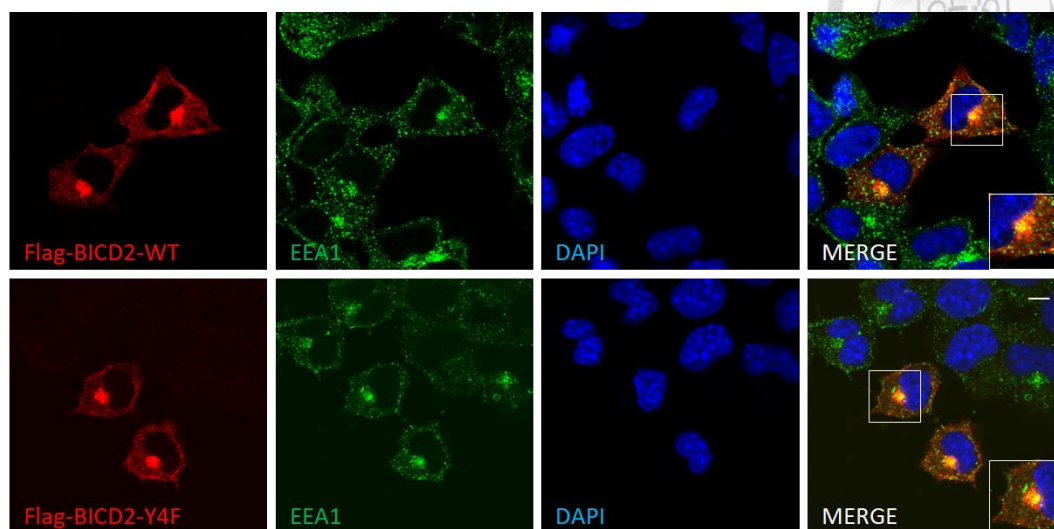(A) N2a cells were transiently transfected with Flag-BICD2-WT or Flag-BICD2-Y4F. After transfection 24 hours, cells were immunostained with anti-Flag (red) and anti-GM130 (cis-Golgi) (green) antibodies. Nuclei were stained by DAPI (blue). Scale bar:5 μm.

(B) N2a cells were transiently transfected with Flag-BICD2-WY or Flag-BICD2-Y4F. After transfection 24 hours, cells were immunostained with anti-Flag (red) and anti-TGN46 (trans-Golgi) (green) antibodies. Nuclei were stained by DAPI (blue). Scale bar:5 μm.
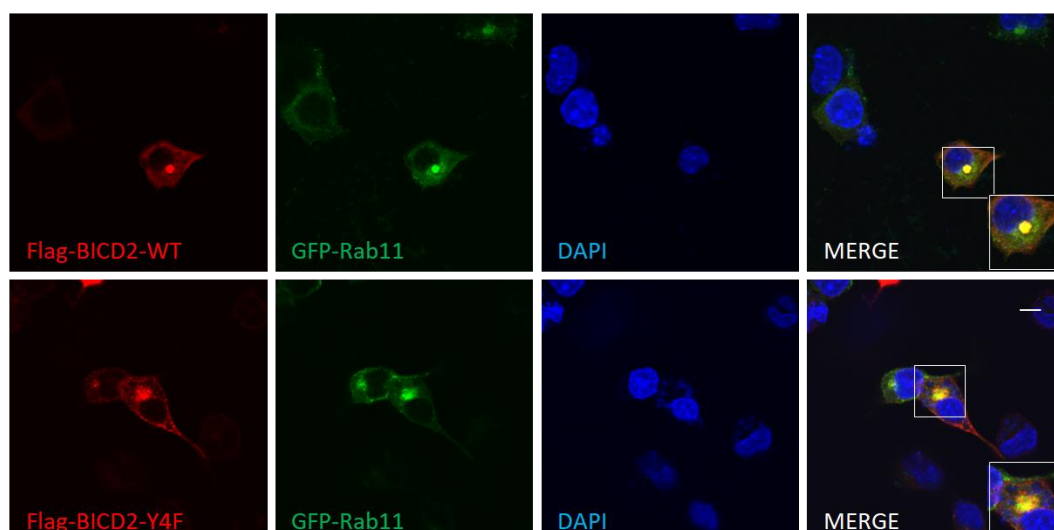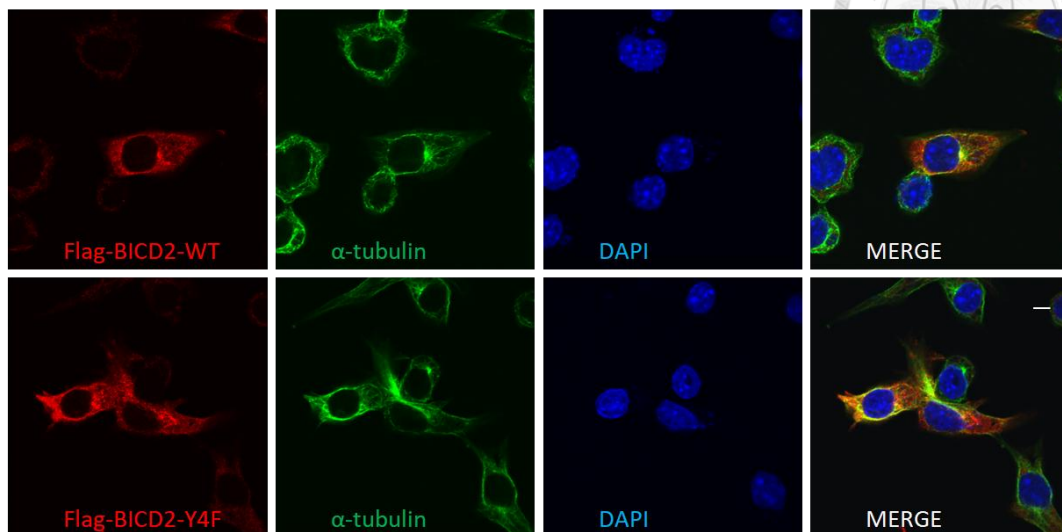
A.

B.

Figure 8. BICD2-Y4F mutant does not affect the subcellular location

(A) N2a cells were transiently transfected with Flag-BICD2-WT or Flag-BICD2-Y4F. After transfection 24 hours, cells were immunostained with anti-Flag (red) and anti-EEA1 (early endosome) (green) antibodies. Nuclei were stained by DAPI (blue). Scale bar:5 μm.

(B) N2a cells were transiently cotransfected Flag-BICD2-WT or Flag-BICD2-Y4F with GFP-Rab11 (recycling endosome). After transfection 24 hours, cells were immunostained with anti-Flag (red) antibody. Nuclei were stained by DAPI (blue). Scale bar:5 μm.

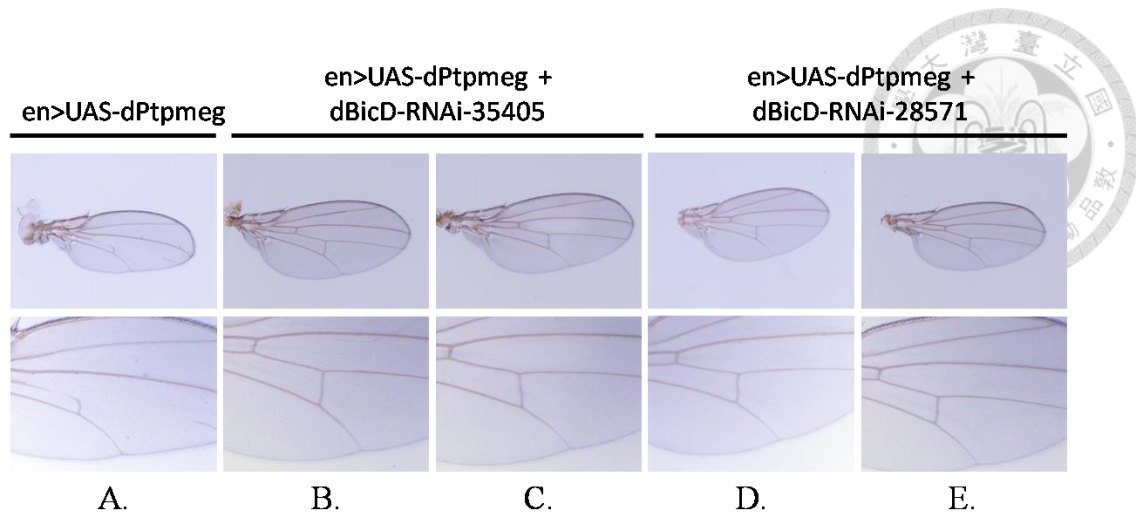**Figure 9. BICD2-Y4F mutant affects the microtubular structure**

N2a cells were transiently transfected Flag-BICD2-WT or Flag-BICD2-Y4F. After transfection 24 hours, cells were immunostained with anti-Flag (red) and anti-αtubulin (green) antibodies. Nuclei were stained by DAPI (blue). Scale bar:5 μm.
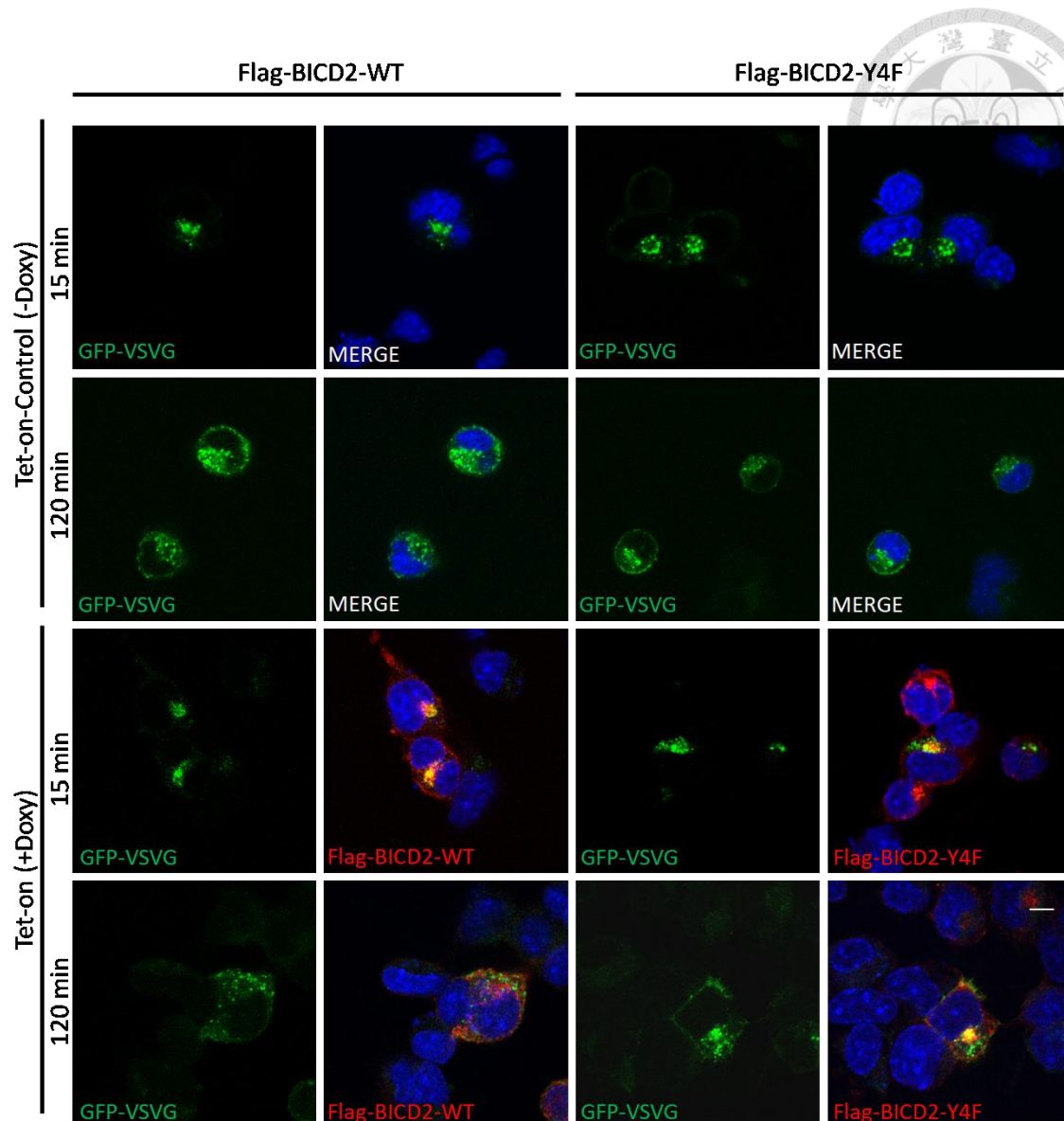
Figure 10. BICD2-Y4F mutant does not have defects in the anterograde transport of VSVG

The inducible expression Flag-BICD2-WT or Flag-BICD2-Y4F N2a cell lines were used. To express Flag-BICD2-WT or Flag-BICD2-Y4F, cells were treated with doxycycline (10μg/ml) for 24hrs, then trasnfected with GFP-VSVG to perform VSVG transport assay. The temperature shift 15 minutes as control. Cells were immunostained with anti-Flag (red) antibody. Nuclei were stained by DAPI (blue). Scale bar:5 μm.

| en>UAS-dPtpmeg | en>UAS-dPtpmeg + dBicD-RNAi-35405 | | en>UAS-dPtpmeg + dBicD-RNAi-28571 | |
| A. | B. | C. | D. | E. |

Figure 11. dPtpmeg and dBicD have genetic interaction, dBicD deletion rescues the wing vein loss defects caused by dPtpmeg

(A)en>UAS-dPtpmeg ,ectopically expression of dPtpmeg in Drosophila wings causes the wing vein missing defects. (B) and (C) en>UAS-dPtpmeg;dBicD-RNAi^{GC}, rescue the wing vein loss defects. (D) and (E) en>UAS-dPtpmeg;dBicD-RNAi^{HM}, rescue the wing vein loss defects.
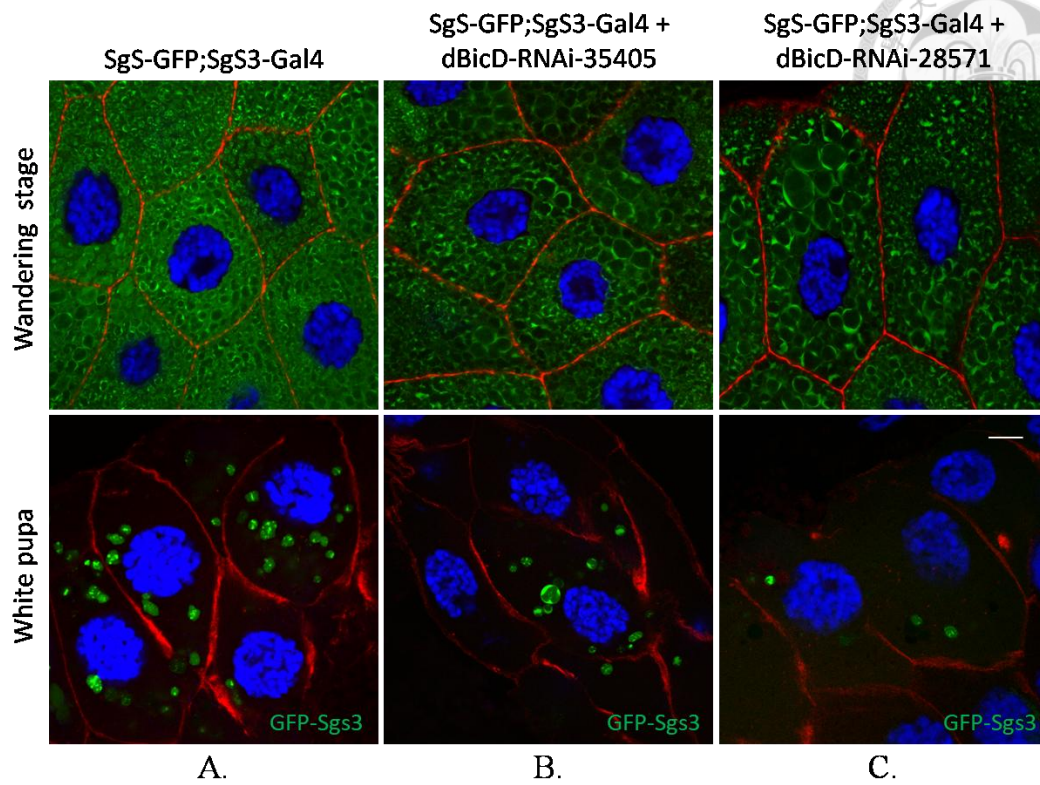
Figure 12. The role of dBicD in fly salivary gland

(A)SgS-GFP;SgS3-Gal4. (B) SgS-GFP;SgS3-Gal4> dBicD-RNAi^{GC}.

(C) SgS-GFP;SgS3-Gal4> dBicD-RNAi^{HM}. Palloidin were stained in red. Scale bar:15 μm.